POLITECNICO DI TORINO

Master's Degree in Ingegneria Biomedica

Politecnico di Torino

Master's Degree Thesis

Multicenter Study on Conduction Block Estimation in Chronic Inflammatory Demyelinating Polyneuropathy and Multifocal Motor Neuropathy using Compound Muscle Action Potential Deconvolution

Supervisor: Prof. Luca MESIN

Co-supervisor: Dr. Dario COCITO

Candidates: Valeria Giampani

Myriam Ganci

2025

ABSTRACT

This thesis presents a deconvolution method for estimating conduction block (CB), i.e., the failure of the action potential (AP) to propagate along the axon of a motor neuron. The classic methods used in clinical practice are based on estimating the area and amplitude of two compound action potentials (CMAPs) recorded by transcutaneous electrical stimulation of a nerve at sites distal and proximal to the nerve segment where conduction block is suspected. However, these estimates are sensitive to phase cancellations due to the temporal dispersion of the MUAPs constituting the CMAP. In subjects with neuropathies, temporal dispersion is abnormal due to impairment of the myelin sheath, which causes a marked reduction in conduction velocity. The proposed procedure consists of deconvolving the CMAPs and provides the delay distributions, which are convolved with a kernel representative of the waveform to approximately reconstruct the CMAPs. The slow afterwave of the muscle potentials was included in the kernel; in addition, the integral of the delay distributions was used to obtain the CB estimate. The method was tested on experimental signals obtained from subjects with two diseases: chronic inflammatory demyelinating polyneuropathy (CIDP) and multifocal motor neuropathy (MMN). The approach is less affected by phase cancellations than conventional methods, allowing for a more stable estimation of conduction block. However, it has been shown to be quite sensitive to various experimental variables, such as measurement quality, stimulation level, electrode placement, and correct indication of limb length. This is because deconvolution, being an inverse operation, is affected by inaccuracies in the tracings and measurement conditions. In the future, the method could be optimised by improving the standardisation of acquisition conditions. It would be useful to record supramaximal tracings, immobilise the limb during measurement, and digitise clinical tracings, as paper tracings make it difficult to obtain accurate estimates. These measures would reduce uncertainty and provide a more reliable and reproducible estimate of conduction block.

Table of contents

List of tables

List of figures

3.3 Distal and proximal CMAPs together with the kernel used for deconvolution. The slow afterwave (SAW) appears as a slow return to baseline following the main negative peak and is included in the kernel model.

3.4 Exponential fitting of the distal CMAP.

3.5 Comparison between initial kernel (black) and optimal kernel (magenta).

3.6 Comparison between distal CMAP (red), old kernel (green), new kernel only with hermite (magenta) and new kernel with hermite+function (blue).

3.7 Original trace from the medical records provided by neurologists.

3.8 Digitalised signal with the procedure described above.

3.9 Example of final digitalised signal

4.1 CMAP recorded by stimulating the peroneal nerve in the head of the fibula and the popliteal fossa. A distal distance of 100 mm and a proximal distance of 450 mm were set.

4.2 CMAP recorded by stimulating the median nerve in wrist and elbow. A distal distance of 80 mm and a proximal distance of 250 mm were set.

4.3 CMAP recorded by stimulating the median nerve in wrist and axilla. A distal distance of 80 mm and a proximal distance of 330 mm were set.

4.4 The exponential fitting performed to model the return to baseline of the distal CMAP is shown.

4.5 The slow afterwave model appropriately reflects the negative phase and return to baseline of the distal CMAP.

4.6 This figure shows the Landweber reconstruction for both proximal and distal stimulation. It is possible to observe the high reconstruction accuracy, as the signal morphology is sufficiently well preserved.

4.7 The distribution of delays in the two CMAPs, distal (in blue) and proximal (in red), supports the theory of no conduction block. The proximal response partially intersects with the distal response, suggesting an almost immediate proximal response to the distal response.

4.8 In the figure above, both the baseline shift process and the removal of the final drift present in the original signal, which would have disrupted the proposed method, have been applied.

4.9 The procedure described in Fig. 4.8 was also applied to the proximal CMAP.

4.10 This figure shows the Landweber reconstruction for both proximal and distal stimulation.

4.11 The distal (blue) and proximal (red) delay distributions highlight the presence of conduction block, which, using the deconvolution method, can be seen in the delayed response of the proximal compared to the distal. With classical methods, a reduction in the area and amplitude of the proximal is noted, indicating the presence of CB. The best accuracy is obtained with the deconvolution method.

Chapter 1: Introduction

Peripheral neuropathies are group of disorders damaging the peripheral nervous system. Clinically, the symptoms include weakness, sensory loss and reduced reflexes, while from an electrophysiological point of view the main characteristic that affect these conditions is the conduction block (CB), defined as the failure arrest of action potential to propagate in structurally intact motor axons.

Chronic Infiammatory Demyelinating Polyneuropathy (CIDP) and Multifocal Motor Neuropathy (MMN) are two treatable rare neuropathies, but they are often challenging to diagnose.

This thesis builds upon a deconvolution-based approach originally proposed by Prof. Luca Mesin, which aims to overcome the limitation of phase cancellation that the traditional methods used in clinics through nerve conduction studies (NCS), such as amplitude and area, have. Conventional methods rely on comparing compound muscle action potentials (CMAPs) evoked by stimulating the same nerve at two distinct sites—distal and proximal—and interpreting amplitude or area reductions as indicators of conduction block. However, these measurements are highly sensitive to phase cancellations caused by temporal dispersion of individual motor unit action potentials (MUAPs). Such dispersion, especially pronounced in demyelinating conditions, leads to waveform distortions that can mimic or mask a true conduction block, compromising diagnostic accuracy. In this work, we extend Prof. Mesin's method to a multicenter study, thanks to the collaboration with Dr. Dario Cocito (A.O.U. Città della Salute e della Scienza di Torino, "Le Molinette") and Dr. Pietro Doneddu (IRCCS Humanitas, Milan). With to their contribution, we collected a large and heterogeneous dataset of electrophysiological recordings from patients diagnosed with CIDP and MMN. The method models each CMAP as the convolution between a kernel function—representing the stereotyped MUAP waveform—and a distribution of conduction delays that reflects the spread of conduction velocities along the nerve. Through deconvolution, we can estimate this distribution and evaluate the proportion of motor fibers failing to transmit impulses between distal and proximal stimulation sites. The present work focuses on motor nerves routinely tested in clinical practice: the median, ulnar, peroneal, tibial, and occasionally the radial and femoral nerves. These nerves provide a comprehensive overview of both upper and lower limb conduction properties. Each nerve was evaluated through standard NCS protocols, using supramaximal electrical stimulation at defined distal and proximal sites, and recording CMAPs from target muscles. The deconvolution method was then applied to pairs of signals to estimate delay distributions and quantify the percentage of conduction block.

Although deconvolution offers clear theoretical and practical advantages, in practice its accuracy still depends on a number of small but crucial experimental factors. Electrode stability, the correct measurement of limb length, the ability to reach a truly supramaximal stimulus and also pain tolerance that varies widely from patient to patient, all make a difference. In those cases, stimulation must be limited, and the result is a less-than-perfect CMAP response. Keeping the limb still is another subtle but important issue — even tiny movements can distort the waveform enough to complicate later analysis. Finally, factors such as digitization accuracy,

electrode-skin impedance, and differences in equipment calibration between laboratories add further variability that can be hard to control completely. However, by reducing the confounding effect of phase cancellation, deconvolution method may offer a complementary or alternative diagnostic criterion to traditional amplitude and area methods.

The following chapters will describe the physiological background of peripheral nerve conduction, the theoretical framework of the proposed method, and the results obtained from its application to the multicenter dataset.

1.1 Physiology of the Peripheral Nervous System (PNS)

Rare neuropathies are diseases of the peripheral nervous system (PNS) - basically all those nerves branching out from the brain and spinal cord, connecting the CNS with the rest of the human body. The PNS has two main jobs: the somatic part handles voluntary movements and sensory perception, while the autonomic part regulates involuntary functions. The autonomic system is itself composed by sympathetic and parasympathetic branches working as opposite forces keeping everything balanced - that's homeostasis. [1]

From a structural point of view, peripheral nerves are long bundles of axons surrounded by myelin, an insulating sheath made by Schwann cells. This layer enables rapid and efficient conduction of electrical impulses through a process known as saltatory conduction. Interruptions in the myelin sheath, called the nodes of Ranvier, are densely populated with voltage-gated sodium (Na_v) channels. At these sites, the action potential (AP) is regenerated and “jumps” from one node to the next, allowing the signal to travel much faster along the nerve fiber.

This mechanism provides two major physiological advantages:

1. Speed – Conduction velocity can reach up to 150 m/s in large, myelinated fibers, compared with only 0.5–10 m/s in unmyelinated ones. [2]
2. Metabolic efficiency – Because ion exchange occurs only at the nodes, energy consumption by sodium–potassium pumps is minimized, reducing the overall metabolic cost of conduction.

The AP travels down the motor neuron axon following this fast mechanism until it reaches the neuromuscular junction (NMJ) - a small synaptic gap where the nerve terminal meets the muscle fiber. The NMJ works as a chemical synapse, which means the neuron's electrical signal must get converted into a chemical one to activate the muscle. It is basically the interface that lets nerve and muscle cells communicate.

When the AP hits the nerve terminal, voltage-gated calcium channels open and let Ca^{2+} enter in the pre-synaptic cleft, triggering the release of acetylcholine (ACh). ACh is a neurotransmitter that binds to receptors on the muscle membrane, causing the depolarization that generate a muscle action potential - and that leads to contraction. This process explains how a neural signal activates a single muscle fiber; in physiological conditions motor neurons do not operate on isolated fibers but on groups of them.

In fact, each skeletal muscle fiber is innervated by just one motor neuron branch, but that same motor neuron can branch out and control multiple muscle fibers. One motor neuron plus all its muscle fibers makes up a motor unit (MU), whose size varies a lot depending on what the muscle does. Muscles needing precise control might have just a few fibers per unit, while powerful muscles can have hundreds.

This is a crucial point, because the electrophysiological signals we record in clinical settings reflect many MUs working together, not individual fibers. In nerve conduction studies, the compound muscle action potential (CMAP) is what gets measured - it's the combined electrical activity from multiple motor units firing at once, generated as APs propagate along the nerve.

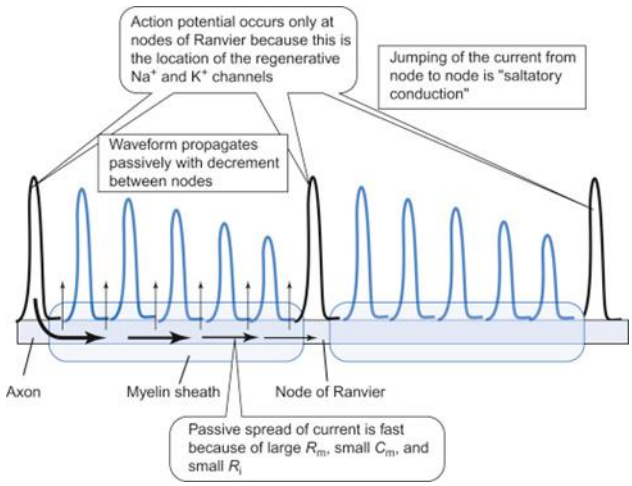

Figure 1.1. *Saltatory conduction along a myelinated axon – APs are regenerated only at the nodes of Ranvier, where voltage-gated sodium and potassium channels are concentrated. Between nodes, the current spreads passively with decrement through the myelinated internode, allowing rapid and energy-efficient propagation.*

So, if the integrity of the myelin sheath is compromised, this procedure fails, and the propagation of APs becomes slower or in some cases it is blocked. To verify if nerve conduction is working correctly, clinicians do electrophysiological examinations such as nerve conduction studies (NCS) and electromyography (EMG).

1.2 Principles of Electrophysiology (EDX)

Electrical signals coming from the mechanism described in 1.1 can be measured and analysed as a diagnostic tool to detect abnormalities. The electrodiagnostic (EDX) is a clinical exam that combines two types of tests that are commonly used: electromyography (EMG) and nerve conduction studies (NCS). Both tests are important in evaluating injuries or diseases of nerves and muscles, determining the severity and their eventual progression over the time.

Before the electrophysiological tests, the clinician asks the patient routine questions to get an overview of the perceived symptoms. Common questions to get a detailed patient medical history are related to the percept weakness and that can take to the difficulty in performing everyday tasks

- a classical question is if they can lift a grocery bag or open a bottle – or to the pain, fatigue, gait disturbances, or also asymmetry in these problems.

This first evaluation allows the doctor to have some initial suppositions which will then be confirmed with subsequent tests, involving both muscles and nerves.

Electromyography (EMG) evaluates the electrical activity of the muscles. It can be thought as a method that enables the muscle to "speak," translating it into measurable electrical signals. The examination is performed by inserting a fine needle electrode through the skin and into the muscle of interest; this electrode acts both as a sensor and as a microphone, detecting the electrical potentials generated by muscle fibers during rest and contraction.

The insertion of this pin can cause discomfort or pain for the patient, as the electrode penetrates the muscle tissue and must often be repositioned in different anatomical sites to sample various motor units. When the muscle is completely relaxed, a healthy muscle shows no spontaneous electrical activity, resulting in a silent baseline. During voluntary contraction, the patient has to gradually activate the muscle: the electrical activity increases proportionally to the degree of contraction, and this can be both visualized on the oscilloscope and heard as an audible signal — a characteristic “crackling” or “interference” sound that reflects the summation of motor unit action potentials. The more complex this interference pattern becomes, the more motor units are being recruited, indicating an appropriate neuromuscular response. From an engineering standpoint, EMG signals are rich in temporal and spectral features that can be quantitatively analysed [3].

Nerve conduction studies are usually done along with EMG and record how nerves are functioning. During this procedure, electrodes are taped on the skin surface along the nerve pathway. Electrical signals are then sent along the pathway. Sensors record the electric activity and measure how fast the impulse travels along the nerve pathway. The results are displayed on a computer monitor and are evaluated. In NCS, electrical stimuli are applied to peripheral nerves and responses are recorded from either the nerve itself or from the muscle it innervates. The main parameters analyzed are latency, conduction velocity, and amplitude of the response. Each parameter provides insight into different aspects of nerve function. Prolonged latency and reduced conduction velocity are typically linked to demyelination, since the loss of myelin slows the propagation of the action potential. A drop in CMAP amplitude or area after proximal compared to distal stimulation, despite preserved conduction velocity, defines a conduction block and reflects the inability of impulses to traverse a demyelinated or dysfunctional segment. By contrast, a generalized reduction in CMAP amplitude across all stimulation sites is characteristic of axonal loss, because fewer fibers remain available to transmit signals. Nerve conduction studies (NCS) may be diagnostically helpful in patients suspected of having almost any PNS disorder and represent an extension of the neurological examination. NCS involve activating nerves electrically with small safe pulses over several points on the skin of the limbs and measuring the responses obtained [4].

They provide objective and quantitative information on the functional status of peripheral nerves, allowing the clinician to distinguish between axonal and demyelinating pathologies.

A reduction in conduction velocity is generally indicative of a neuropathic process. In clinical practice, an arbitrary threshold is commonly used: a median nerve motor conduction velocity

below 38 m/s is considered abnormal. In severe axonal neuropathies, conduction velocity may also decrease as the fastest-conducting fibers are affected; however, it rarely falls below 38 m/s [5].

The presence of intermediate conduction velocities in certain hereditary neuropathies, and the fact that some genetic mutations (for example, in the P0 gene) can produce either axonal or demyelinating phenotypes, complicate what would otherwise be a clear diagnostic distinction [6]. In routine nerve conduction studies (NCS), responses are elicited by supramaximal electrical stimuli with a pulse duration of 0.1–0.2 ms [7]. The resulting compound muscle action potential (CMAP) represents the summated electrical response of multiple motor units. The amplitude, shape, and latency of the CMAP depend on the number and functional state of the activated nerve fibers. As stimulus intensity increases, additional motor fibers are recruited, leading to a progressive rise in amplitude until a plateau is reached, corresponding to the activation of all large, myelinated fibers [7,8].

One of the most common neuropathies of the upper limb is the carpal tunnel syndrome (CTS), that affect people who do jobs which involve the repetitive or prolonged movement of the wrist, resulting in the compression of the median nerve in the tract of the carpal tunnel at the wrist.

So, the median motor nerve is stimulated through NCS in two landmarks, whose are distally the wrist and proximally the elbow, and the response is recorded with surface electrodes over the abductor pollicis brevis (APB) muscle. Distal latency, amplitude, and conduction velocity are measured to evaluate whether conduction is preserved, slowed, or blocked along the tested segment.

This approach not only detects the presence of neuropathy but also helps classify it as primarily demyelinating or axonal, which is critical for guiding further diagnostic and therapeutic decisions.

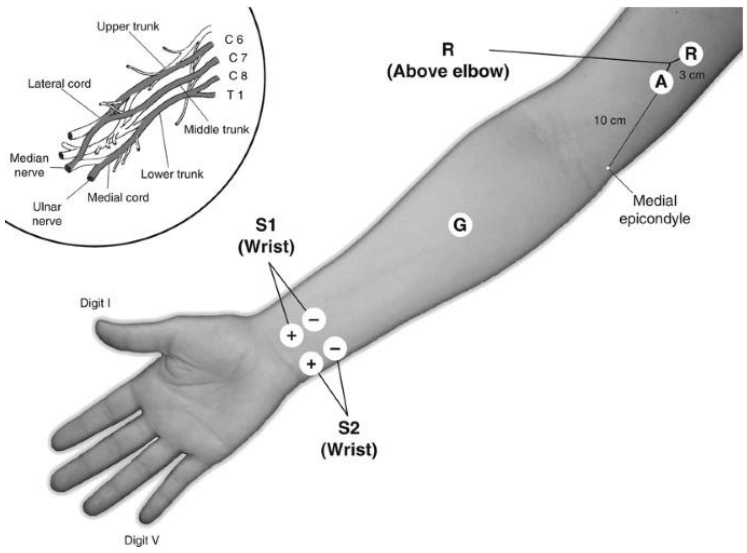

Figure 1.2 *Example of motor nerve conduction study – Electrode placement for median nerve stimulation at the wrist and above the elbow. Recording electrodes are positioned over the abductor pollicis brevis muscle, while ground and reference electrodes complete the setup. The inset shows the brachial plexus anatomy and origin of the median and ulnar nerves.*

In the present work, electrophysiological recordings were performed on several major motor nerves of the upper and lower limbs. A concise anatomical overview of these nerves is therefore provided below to facilitate the interpretation of subsequent electrodiagnostic findings.

1.2.1 Anatomical overview of the studied motor nerves

The nerves that are routinely examined in electrodiagnostic practice are the median, ulnar, radial, peroneal, tibial, and femoral nerves.

The median nerve originates from the brachial plexus (roots C5–T1) through the union of its medial and lateral cords. [8, 9] It travels along the anterior aspect of the arm and forearm and enters the hand through the carpal tunnel. Functionally, it supplies most forearm flexor muscles and part of the thenar eminence, including the abductor pollicis brevis, which is commonly used as the recording site in motor nerve conduction studies. Stimulation is typically applied at the wrist and elbow to calculate conduction velocity. The elbow is particularly useful because the nerve runs superficially in the antecubital fossa, allowing easy and reproducible stimulation. Sometimes are used additional proximal sites, such as the axilla or Erb point, to investigate the more proximal segments. The ulnar nerve is the other major motor nerve of the upper limb. It arises from the medial cord of the brachial plexus (roots C8–T1) and runs along the medial side of the arm and forearm into the hand. It primarily controls the intrinsic muscles of the hand. For motor conduction studies, stimulation is applied at the wrist, below the elbow, and above the elbow. These three sites make it possible to analyse conduction across the segment that passes behind the medial epicondyle, the region most frequently investigated for focal slowing or conduction block. The radial nerve, originating from the posterior cord of the brachial plexus (C5–C8), and follows a posterior course along the arm and forearm. It provides motor input to the extensor muscles of the wrist and fingers.

In the lower limb, the peroneal nerve (roots L4–S2) courses around the fibular head, where it can be stimulated easily; the tibial nerve (roots L4–S3) runs down the posterior leg and can be stimulated at the ankle and popliteal fossa. Finally, the femoral nerve arises from the lumbar plexus (roots L2–L4) and supplies the anterior thigh muscles, mainly the quadriceps femoris; stimulation is typically applied near the inguinal region.

1.3 Compound Muscle Action Potential (CMAP)

The compound muscle action potential (CMAP) is among the first recorded waveforms in clinical neurography and one of the most common in clinical use. It is derived from the summated muscle fiber action potentials recorded from a surface electrode overlying the studied muscle following stimulation of the relevant motor nerve fibres innervating the muscle. Surface recorded motor unit potentials (SMUPs) are the fundamental units comprising the CMAP. [10].

From a physiological standpoint, generating a CMAP involves several steps that happen in sequence: the action potential conducts along motor axons, neurotransmitter gets released at the neuromuscular junction, and the muscle fiber membrane depolarizes, leading to contraction. Each

step shapes the recorded signal in different ways. Latency includes both the time for nerve conduction and the delay at neuromuscular transmission; amplitude is proportional to how many muscle fibers depolarize; duration reflects how synchronized the activated motor units are.

Since CMAP characteristics depend directly on axon integrity, myelin condition, neuromuscular transmission quality, and muscle fiber health, changes in its morphology reveal a lot about what's going wrong in peripheral nerve and motor unit disorders.

1.3.1 Recording methodology

To record the CMAP, the stimulating current or voltage is gradually increased until a point is reached where an increase in stimulus produces no increment in CMAP amplitude. It is only at this (supramaximal) point that reproducible values for CMAP amplitude and the latency between the stimulus and the onset of the CMAP can be recorded accurately. The CMAP amplitude is measured from baseline to negative peak (the neurophysiological convention is that negative voltage is demonstrated by an upward deflection) and measured in millivolts (mV) [4]. Latency, on the other hand, is defined as the time interval between the stimulus artifact and the onset of the CMAP. Its value will be greater for proximal stimulation compared to the distal one because of the longer distance between the stimulating and recording electrodes. The latency difference reflects the conduction time of the fastest nerve fibers between the two stimulation sites, since neuromuscular transmission and muscle activation remain identical for both points of stimulation.

A further difference between distal and proximal stimulation lies in CMAP amplitude. The proximally evoked CMAP is often slightly smaller than the distal one, because of physiological temporal dispersion and partial phase cancellation. However, when the reduction is disproportionate and exceeds the expected physiological variability, it becomes a pathological sign, strongly suggesting the presence of a conduction block.

Measuring the distance between the two shocks we can calculate how fast the nerve transmit (from the knee to the ankle for example). The comparison between proximal and distal stimulation sites provides an objective measure of nerve conduction efficiency and integrity.

1.3.2 Electrodiagnostic correlates of weakness

Among the various symptoms that bring patients to electrodiagnostic evaluation, weakness represents the most relevant functional impairment. From an electrophysiological perspective, the parameter that most directly reflects weakness is the amplitude of the compound muscle action potential (CMAP). While alterations in conduction velocity or distal latency are important diagnostic markers, they do not in themselves explain muscle weakness. Instead, weakness arises when action potentials fail to depolarize muscle fibers, either because axons are lost or because conduction is blocked along a demyelinated segment. [11]

In cases of axonal loss, CMAP amplitudes are reduced at all stimulation sites, reflecting the decreased number of functioning motor fibers. By contrast, in conduction block, axons are preserved but the impulse cannot cross the demyelinated region, resulting in failure of transmission

despite structurally intact fibers. Partial demyelination, on the other hand, may only slow conduction without completely preventing activation of the target muscle.

Thus, CMAP amplitude serves as a functional bridge between physiological measurements and clinical weakness.

1.3.3 Clinical measurements

Quantitative analysis of motor responses in nerve conduction studies is based on several key parameters, each reflecting different physiological aspects of nerve and muscle function.

- Latency is the interval between the stimulus artifact and the onset of the CMAP. Distal latency, usually measured at a fixed distance from the recording electrode, includes not only the conduction time of the fastest motor fibers, but also neuromuscular transmission (around 1 ms) and the initiation of muscle fiber action potentials. Because it reflects only the earliest-activated fibers, latency alone cannot be used to assess the overall severity of a lesion. Extremely short latencies are not physiological and are usually the result of technical errors or anatomical variation, since conduction can be slowed in disease but never accelerated beyond normal limits.
- Conduction velocity (CV) is one of the most widely used parameters. It is obtained by stimulating the nerve at two points and dividing the distance between them by the difference in response latencies:

$$CV = \frac{Distance\ between\ stimulation\ sites}{Proximal\ latency - Distal\ latency}$$

This formula compensates for the constant delays caused by synaptic transmission and muscle activation, allowing the conduction time along the examined segment to be isolated. In certain situations, a residual latency can also be calculated:

$$RL = \text{Distal latency} - \frac{\text{Distance}}{\text{Proximal conduction velocity}}$$

which represents the component of the distal latency not explained by conduction along proximal fibers. Physiologically, conduction velocity depends mainly on axonal diameter, with larger fibers transmitting more rapidly. In human motor nerves, typical conduction velocities range between 35 and 60 m/s [12], while the largest diameter myelinated fibers may conduct at speeds up to ~150 m/s [2]. Variability among fibers produces a small amount of temporal dispersion, which can become more marked in demyelinating neuropathies, leading to longer duration and reduced amplitude of CMAPs.

- Amplitude is usually measured from the baseline to the negative peak of the CMAP and expressed in millivolts. It reflects the number of activated muscle fibers and, by extension, the number of functional motor axons. Because it is directly related to motor unit loss, amplitude is the parameter that correlates most closely with clinical weakness. However,

it is also sensitive to electrode placement and technical variability, so comparisons with the contralateral side are often necessary.

- Area corresponds to the negative portion of the waveform under the baseline. Unlike amplitude, which emphasizes synchronous contributions, area includes both early and delayed components of the CMAP, making it less affected by temporal dispersion. For this reason, it is considered a more stable indicator of the total number of conducting fibers, even though its measurement is performed automatically by the recording equipment due to the difficulty of manual calculation.
- Duration is defined as the time between the onset of the CMAP and its return to baseline. It reflects the spread of conduction velocities among motor fibers: the greater the variability, the longer the CMAP duration. In pathological conditions such as demyelinating neuropathies, the duration of the potential is usually prolonged, and the waveform may present an increased temporal dispersion. Notably, although the amplitude often decreases in these cases, the total area may remain relatively preserved because the delayed components still contribute to the overall response

Taken together, these parameters provide complementary information. [13] Their combined interpretation allows clinicians to distinguish between axonal and demyelinating pathologies, to detect conduction block, and to quantify the severity of peripheral nerve dysfunction.

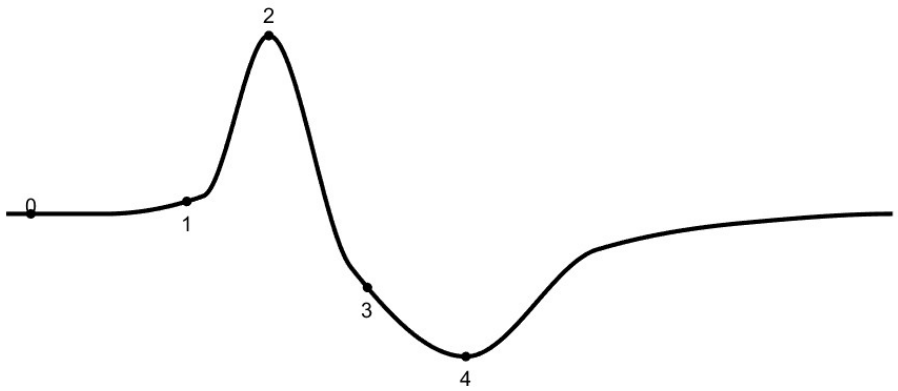

Figure 1.3 *Example of a CMAP waveform with main measurable parameters.*
0–1 = latency; 1–3 = peak duration; 2 = peak amplitude; 2–4 = total amplitude

Chapter 2: Rare neuropathies

After establishing the physiological and diagnostic background, attention turns to the pathological conditions of interest in this study. The thesis examines electrophysiological signals from patients with Chronic Inflammatory Demyelinating Polyradiculoneuropathy (CIDP) and Multifocal Motor Neuropathy (MMN) - both rare immune-mediated neuropathies. These conditions usually respond well to immunotherapy and are treatable but diagnosing them can be difficult. That's why accurate clinical and electrodiagnostic evaluation matters so much.

For a good diagnosis and effective treatment, it is essential to correctly classify neuropathy through symptoms and electrodiagnostic tests, which together allow the clinician to determine whether the damage is axonal or demyelinating.

Common causes of peripheral neuropathy include diabetes mellitus, nerve compression or trauma, and hereditary diseases affecting axon or myelin structure. Infections, toxins, autoimmune disorders, and systemic diseases can also be involved.

Early symptoms typically involve sensory changes that are progressive and symmetrical - loss of sensation, numbness, pain, or burning feelings. In more advanced cases, symptoms may extend proximally and include numbness of the proximal regions and significant functional impairment. [1]

2.1 Axonal and demyelinating lesions

From a pathophysiological point of view, peripheral neuropathies are classified into two categories: demyelinating neuropathies and axonal neuropathies, based on the nerve structure primarily involved in the pathological process.
Axonal loss lesions are the most frequently identified pattern in nerve conduction studies. These lesions result from an interruption of the axon, following which its distal portion loses its connection with the cell body, undergoing Wallerian degeneration.
Wallerian degeneration mainly affects the segments of the nerve distal to the lesion and does not manifest itself as an immediate process, but rather as a progressive sequence of events involving the disintegration of the axon and the removal of myelin by Schwann cells.
In nerve conduction studies, axonal loss lesions are evident through a reduction in CMAP amplitude, as fewer functioning motor axons remain connected to muscle fibres. However, the remaining axons continue to conduct normally, as myelin is not directly involved in the pathological process. As a result, latencies and conduction velocities tend to remain within normal limits.
However, as motor fibre loss progresses, large and fast axons are also lost, causing a slight slowdown in nerve conduction parameters.
The abnormalities observed are influenced by the dynamics and timing of axonal damage: in fact, distal motor latency can reach values equal to 120% of the normal limit, while conduction velocity is slightly slowed, to about 80% of the normal limit.
As regards CMAP, a rapid loss of axons leads to a marked reduction in its amplitude. Conversely, if axonal loss is slow, the remaining axons can re-establish the lost muscle innervation by developing new connections with the muscle fibres, thus allowing the CMAP amplitude to remain

within the normal range. However, fibres undergoing regeneration have a lower conduction velocity than the original ones, resulting in a more dispersed CMAP with less synchrony of action potentials. [4]

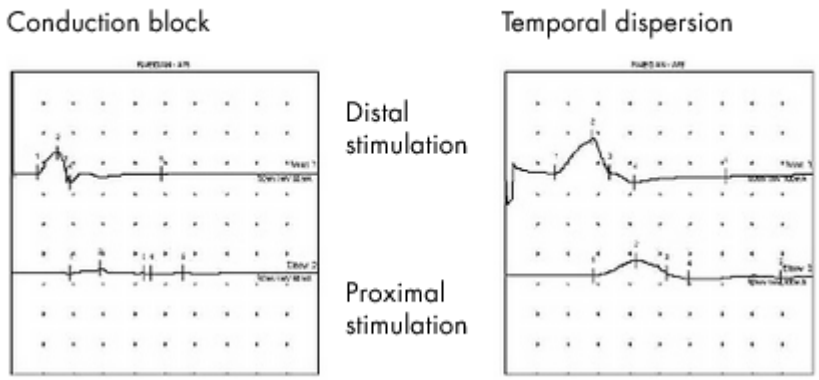

Figure 2.1 *Both tracings show signs of demyelination in motor conduction studies of the median nerve. In the left tracing, there is an almost complete conduction block with no response to proximal stimulation. In the right track, however, there is a time dispersion characterised by an approximately 40% increase in CMAP duration when stimulation is applied proximally. In both conditions, the CMAP amplitude is reduced compared to distal stimulation.*

Demyelination is the interruption of the normal transmission of nerve impulses and, consequently, the failure proper functioning of the nervous system. In particular, nerve conduction is slowed down due to the thinning of the myelin sheath, a phenomenon that leads to an increase in internodal capacitance and conductance. This causes a loss of current along the axonal tract: the current is not sufficient to activate the next Ranvier node, giving rise to a conduction block. In the presence of such a block, there is a failure of saltatory conduction, resulting in a reduction or absence of motor response.

Two main types of demyelinating neuropathies can be distinguished:

- Hereditary neuropathies: these result from genetic alterations and cause widespread demyelination along the entire length of the nerve. Classic examples are Charcot-Marie-Tooth disease (CMT) and hereditary neuropathy with hereditary paralysis (HNPP). [14]
- Acquired neuropathies: these are caused by alterations in the immune system. In these cases, we refer to focal demyelination, as the process selectively affects certain segments of the nerve, causing localised conduction blocks. Acquired neuropathies include those associated with diabetes mellitus or compressive neuropathies, such as carpal tunnel syndrome.

Specifically, demyelinating neuropathies include various pathological conditions, such as acute inflammatory demyelinating polyradiculoneuropathy (AIDP – Guillain-Barré syndrome) and also the two neuropathies considered in this work -CIDP and MMN. [15]

In particular, CIDP is a chronic disease of the PNS which involves a damage in the nerves, in particular to the myelin sheath, blocking the impulse transmission and so the nerves functionality. Patients prove loss of strength, sensibility, and equilibrium, resulting in a gait impairment. It generally affects the regenerating myelin; it is essentially an autoimmune disease against the myelin, that is damaged, the nerves are blocked, so if this attack against myelin is recognised and treated early, nerves remyelinated and recover. This neuropathy has a subacute trend - it gets worse over time. In the past, was treated with cortisone - immunosuppressant that blocks the immune response; however, this is a chronic disease, and corticosteroids have collateral effects, including agitation, glucose intolerance or diabetes, gastritis, and elevated blood pressure.

Furthermore, it is crucial the role of immunoglobulins (IVIG), whose injection allows to block the destruction of antibodies, which is also a well-tolerated treatment for the patient.

Also, MMN is treated with IVIG. The patient affected by MMN has multifocal weakness – so asymmetric – which can affect multiple muscle groups in the body. Thus, in this neuropathy, strong and weak muscle districts coexist for example, the patient may not be able to flex the fingers of his left hand but be able to do this with the right hand - and perhaps not be able to extend them on this side.

In summary, both CIDP and MMN are demyelinating neuropathies that manifests as a significant amplitude drop accompanied by temporal dispersion. As described in paragraph 1.1, myelin plays an essential role in ensuring the effectiveness of saltatory conduction. Therefore, a structural alteration of the myelin sheath, such as that observed in demyelinating processes, causes a slowing down or complete blockage of nerve conduction proportional to the degree of interruption of the myelin sheath.

From an electrophysiological point of view, this manifests as very prolonged motor latencies and slowed conduction velocities, parameters that reflect the slowing of impulse propagation along the fibres. In some cases, when demyelination mainly affects the proximal segments of the nerve, distal motor latency and conduction velocity may be normal, as the distal portions of the nerve remain intact. The uneven slowing of conduction results in pathologically dispersed CMAPs. When assessing conduction block or temporal dispersion, a reduction in CMAP amplitude is observed. In particular, the CMAP area with stimulation proximal to the conduction block site shows a 20% reduction compared to the distal area. Temporal dispersion, which reflects a loss of synchrony in the conduction of individual action potentials, results in a reduction in CMAP amplitude. This occurs due to phase cancellation, in which part of the positive component of the action potential cancels out the negative part of the other. This phenomenon directly reflects the loss of structural integrity of the myelin sheath and the consequent alteration of nerve conduction, constituting an important diagnostic indicator in demyelinating neuropathies. [4]

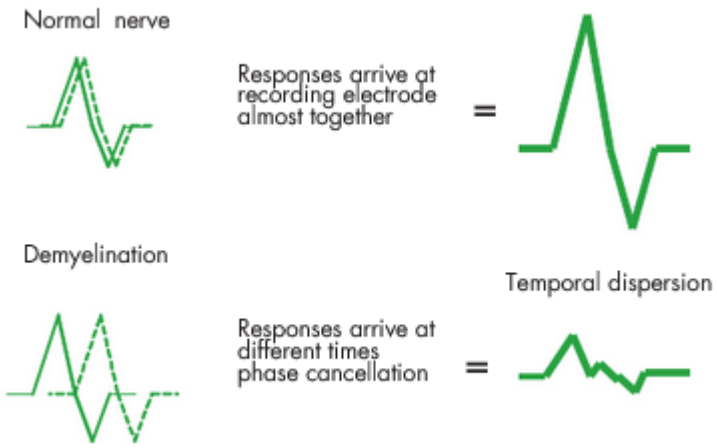

Figure 2.2 *Schematic representation of phase cancellation and temporal dispersion in a demyelination process. In normal nerves, responses are synchronous in time and add up, producing a CMAP with greater amplitude than that of the individual potentials. In the presence of temporal dispersion, responses lose synchrony, resulting in an increase in duration and a reduction in the overall amplitude of the CMAP.*

In the case of autoimmune axonal neuropathies, caused by dysfunction or interruption of voltage-dependent nodal channels, a slowing of conduction velocity can be observed which, when analysed in isolation, may resemble that of demyelinating neuropathies. This slowing appears to be due to a prolongation of the depolarisation time required to reach the action potential regeneration threshold in successive Ranvier nodes.

This condition suggests that conduction slowing is not always a direct consequence of structural damage to the myelin sheath but may result from functional alterations in nodal ion channels, such as those observed in autoimmune processes.

Therefore, in order to avoid misdiagnosis or incomplete interpretations, it is necessary to take these observations into account, which broaden the spectrum of electrophysiological characteristics in some axonal neuropathies. [16]

2.2 Conduction Block

Conduction block is one of the main physiological consequences of demyelination and is characterised by the arrest of action potential transmission along structurally intact axons. This phenomenon occurs when the loss or disorganisation of the myelin sheath compromises the ability of the nerve impulse to propagate from one Ranvier node to the next, even in the absence of an actual interruption of the axon. In functional terms, the nerve is therefore electrophysiologically disconnected.

Conduction block is assessed by comparing a series of parameters of the compound muscle action potential (CMAP) – also known as the “M” potential – obtained by supramaximal percutaneous stimulation of the motor nerve at two different points along its course.

To detect the presence of a conduction block, stimulation is performed both proximally and distally to the suspected lesion site. A supramaximal stimulus activates all motor axons; if conduction is

intact, the action potentials travel along the nerve and reach the muscle, eliciting a complete CMAP response.
When stimulation is applied distal to the block, all motor units are excited, since the action potentials are able to reach the muscle without interruption, resulting in a larger M-wave; when the stimulation is applied proximally, only the axons capable of transmitting beyond the lesion contribute to the CMAP, leading to a reduced amplitude if a conduction block is present. For example, for the study of the median or ulnar nerves, stimulation is performed at the wrist and elbow, respectively, while for the peroneal nerve, stimulation sites at the ankle and head of the fibula are used. The parameters commonly analysed include peak-to-peak amplitude, negative peak amplitude, total duration and maximum CMAP area. A comparison between the responses obtained at the two stimulation points allows the identification of any significant drops in the amplitude or area of the proximal CMAP, indicating a partial or complete loss of impulse transmission along the intermediate segment of the nerve. [17]

One of the main difficulties in clinical neurophysiology is to accurately distinguish conduction block from marked time dispersion, as both conditions manifest themselves as a reduction in the amplitude of the CMAP recorded during proximal stimulation compared to distal stimulation.

With temporal dispersion, amplitude reduction occurs because individual fiber action potentials arrive at different times and partially cancel each other out through phase interference. In true conduction block, the amplitude drop reflects actual transmission failure in a subset of demyelinated fibers—some impulses simply don't get through. Standard electrophysiological criteria define conduction block as a proximal amplitude or area reduction exceeding 20-40% compared to distal, or a proximal duration increase beyond 20% [12,18]. These cutoffs provide a practical reference, though they can be affected by technical variables like temperature, electrode position, and skin impedance, as well as normal anatomical variation.

Despite these limitations, the presence of conduction block or marked time dispersion is considered a highly suggestive sign of focal demyelination.

Their recognition is of considerable diagnostic and therapeutic importance, as it allows demyelinating neuropathies to be distinguished from axonal neuropathies and guides the clinical approach, prognosis and treatment strategies.

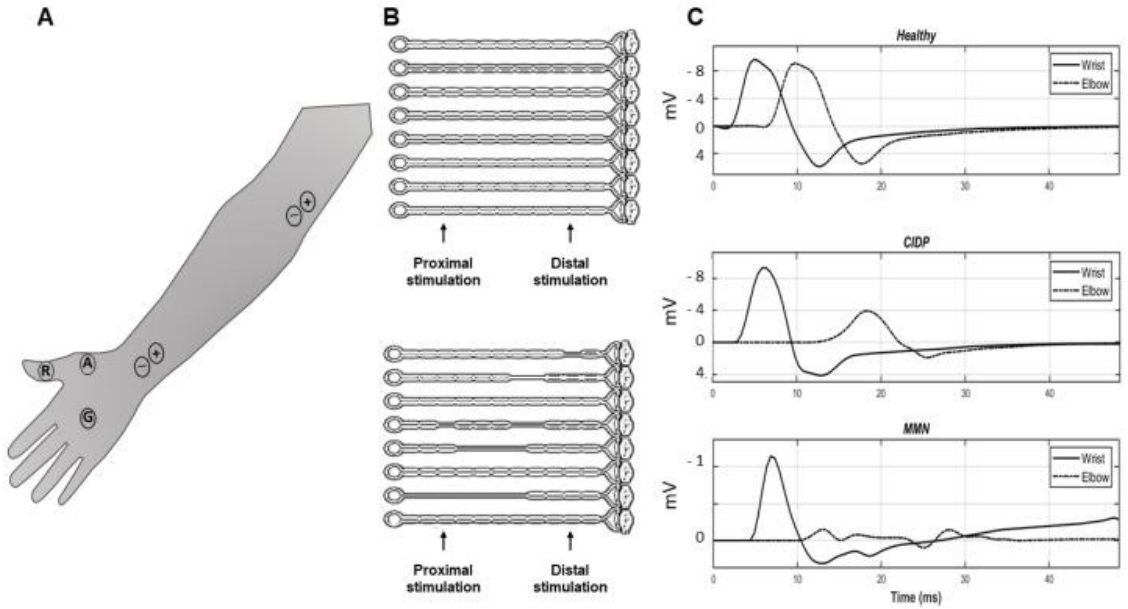

Figure 2.3 *Schematic representation of proximal and distal stimulation in motor nerve conduction studies. (A) Electrode placement on the upper limb.*
(B) Normal (top) and demyelinated (bottom) fibers showing conduction delay and block between stimulation sites.
(C) Example of compound muscle action potentials (CMAPs) recorded at the wrist and elbow in a healthy subject, and in patients with CIDP and MMN, illustrating conduction slowing and block.

2.3 Traditional diagnostic methods

Most of the methods proposed for the estimation of conduction block (CB) are based on a quantitative comparison between compound muscle action potentials (CMAPs) recorded following distal and proximal stimulation of the same motor nerve. As shown in Figure 2.3 [19], in healthy subjects the distal and proximal CMAP waveforms are very similar, except for minor differences related to physiological temporal dispersion. In contrast, in patients with demyelinating neuropathies, the proximal CMAP typically appears reduced in amplitude and area compared to the distal one and exhibits abnormal temporal dispersion, reflecting impaired conduction along the tested nerve segment.

This section describes the amplitude- and area-based methods commonly used in clinical neurophysiology to estimate the presence and severity of conduction block. The severity of CB is evaluated in relation to the number of active motor units (MUs), which is directly proportional to the number of motor axons capable of conducting the impulse. The variation in CMAP amplitude and area between distal and proximal stimulation sites thus provides an estimate of the proportion of fibers with interrupted conduction relative to the total number of fibers stimulated, expressed as a percentage.

Amplitude Method

This method is based on comparing the amplitudes of the proximal and distal CMAPs acquired following nerve stimulation. In pathological cases, focal demyelination or functional interruption of a group of axons causes partial or complete conduction block in some motor fibres. As a result, the corresponding motor units (MUs) are not activated during proximal stimulation, and their responses will not be recorded in the trace. This phenomenon results in a reduction in the amplitude

of the proximal CMAP compared to the distal CMAP, proportional to the number of non-functioning or blocked MUs. An estimate of the severity of CB is provided below in terms of amplitude ratio:

$$Ampiezza = \frac{max(v^{(prox)}(t))}{max(v^{(dist)}(t))} \tag{2.1}$$

Where $v^{prox}(t)$ and $v^{dist}(t)$ are the proximal and distal CMAPs, respectively.

Area method

The method consists of comparing the integrated areas of the distal and proximal CMAPs recorded from the same motor nerve.
In clinical practice, the area is usually computed as the negative phase area, corresponding to the muscle fiber depolarization.
However, in quantitative analyses, the entire CMAP waveform can be integrated to include both the positive and negative phases, according to the following formula:

$$Area = \frac{\int_{tA1}^{tA2} |v_{prox}(t)| dt}{\int_{tB1}^{tB2} |v_{dist}(t)| dt} \tag{2.2}$$

where the integrals are computed over the time intervals corresponding to the duration of each CMAP waveform.

2.4 Limitations of classical methods

As said in 2.3, amplitude and area measurements are the standard clinical approaches for detecting conduction block, but they have limitations. A reduction in proximal CMAP amplitude or area does not always mean true conduction block—other phenomena like conduction slowing, temporal dispersion, or phase cancellation can produce similar changes in the waveform. This is because the recorded CMAP reflects the summation of many individual motor unit action potentials that overlap in both space and time. This summation introduces variations in waveform shape due to overlapping signals, particularly when conduction velocities differ among fibers.

Particular attention should be given to the distinction between conduction block and conduction slowing; this one is results from partial demyelination, where all fibers are still able to conduct, but at a slower velocity. The proximal CMAP appears delayed, with prolonged latency, but the overall response is preserved across all stimulation sites. This mechanism reflects a functional slowing rather than a true transmission failure and should not be misinterpreted as a conduction block.

Temporal dispersion represents another important factor that alters CMAP morphology. It refers to the progressive loss of synchrony among the action potential, caused by differences in conduction velocity among individual nerve fibers. As a result, the compound muscle action potential becomes temporally “spread out”. The morphological effects on the CMAP are an increase in the duration of the waveform and a reduction in the amplitude, while the area is relatively preseverved- at least in the early stages. This effect is considered physiological under normal conditions, but it becomes more evident with the increase of conduction distance and is amplified in demyelinating neuropathies [20].

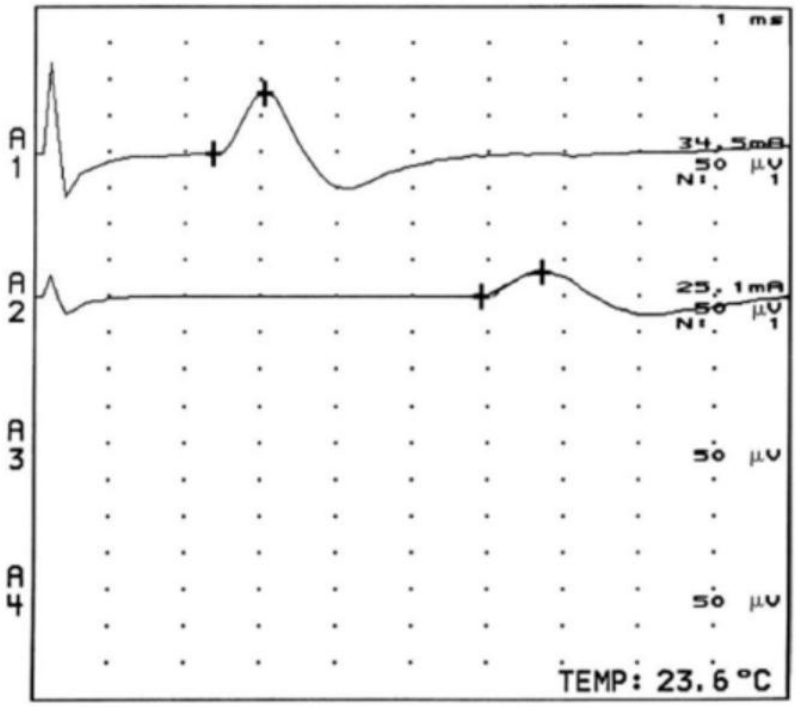

Figure 2.4 *Example of temporal dispersion: the proximal CMAP (A2) shows increased duration and decreased amplitude compared to the distal response (A1), reflecting loss of synchrony among motor fibers.*

Phase cancellation produces even more changes in the recorded waveform, and it is the main cause of the limited reliability of the methods of amplitude and area. It occurs when potentials of opposite polarity overlap, generating destructive interference between positive and negative components. Compared to temporal dispersion, it reduces not only the amplitude but also the overall area of the proximal CMAP and can therefore completely mimic a true conduction block.

In conclusion, it is worth considering one further factor: large motor units, innervated by faster-conducting axons, exert a significant influence on the configuration, amplitude and area of the CMAP. Consequently, the most pronounced phase cancellation effects arise precisely from the dispersion of the activity of these large motor units, which generate high-amplitude action potentials (MUAPs). Therefore, the quantification of conduction block (CB) and temporal dispersion based on CMAP amplitude and area should be interpreted considering which axon

subpopulations are involved in the pathological process. Unfortunately, such information can only be obtained using complex and invasive techniques and, in clinical practice, is generally unavailable during motor conduction studies (NCS).

For all the reasons described above, the next chapter will present a new method for estimating conduction block, based on the application of CMAP deconvolution techniques, which allows for a more accurate and specific assessment of the phenomenon.

Chapter 3: Methode to estimate CB

The following sections describe the mathematical model of the CMAP, the principles of deconvolution, and the implementation of the algorithm used to estimate conduction block from delay distributions.

3.1 CMAP's mathematical model

A compound muscle action potential (CMAP) can be modelled mathematically as the sum of the responses of multiple motor units activated by a supramaximal stimulus. If we define the recorded CMAP as y(t), it can be expressed as:

$$\mathrm{v(t)} = \sum_{\mathrm{n=1}}^{\mathrm{N}} \mathrm{v_n(t - \tau_n)}$$

(3.1)

where N is the number of motor units recruited, $v_n(t)$ is the motor unit action potential (MUAP) of the n-th unit and τ_n represents its conduction delay. These delays reflect the propagation time of action potentials along motor axons and are determined by the distribution of conduction velocities within the nerve. The neuromuscular junction introduces a small and nearly constant synaptic delay, which can be neglected in the model since it affects all motor units equally. When the number of recruited motor units is large, the discrete sum in equation 3.1 can be approximated by a continuous formulation. In this case, the contribution of individual motor units is represented by a continuous delay distribution x(t), where x(t)dt represents the cumulative amplitude of motor units with conduction delays between t and t+dt. This transition from a discrete to a continuous representation is suitable for muscles with a high number of motor units, where individual contributions overlap forming a smooth waveform.

To simplify the problem, it is often assumed that all MUAPs share a common shape but differ in amplitude and temporal delay. Under this assumption, the CMAP can be expressed as the convolution between a kernel function K(t), representing the MUAP waveform, and a delay distribution x(t), representing the probability of observing different conduction times:

$$v(t) \equiv \sum_{n=1}^{N} A_n K(t - \tau_n) = K(t) * \sum_{n=1}^{N} A_n \delta(t - \tau_n) = K(t) * x(t)$$

(3.2)

In this context the Dirac delta functions act as time-shifting operators: each one translates the kernel by the corresponding conduction delay and scales it by an amplitude. Practically, convolution works by shifting the kernel waveform according to each delay value, scaling its amplitude, and adding up all the shifted versions. This means the CMAP we record is actually the sum of multiple time-delayed contributions, not a single waveform.

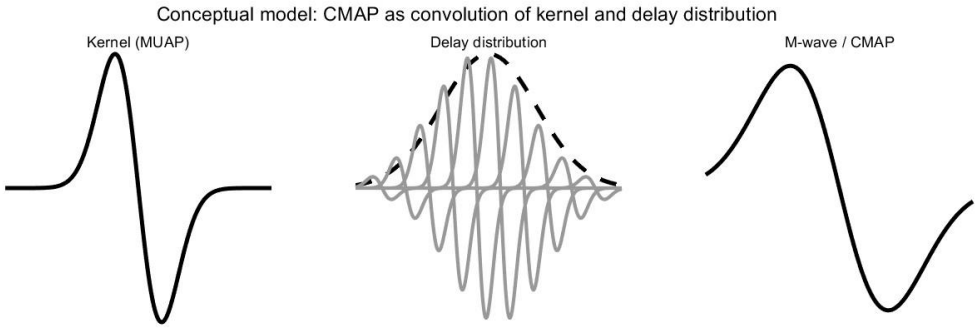

Figure 3.1 *Illustrates this convolution process, showing how the kernel is translated in time and scaled in amplitude according to the delay distribution to form the final CMAP.*

The task is to estimate the underlying delay distribution x(t), which contains the information necessary to characterize temporal dispersion and conduction block.
The delays originate from the propagation of action potentials along different motor fibers, and from the fact that the stimulation is applied at a site distant from the muscle, typically at the wrist or ankle. Each fiber therefore contributes with a slightly different temporal delay.
Depending on the shape of the delay distribution, the superposition of these time-shifted MUAPs produces CMAPs with varying morphology and amplitude — for instance, a wider delay distribution results in a more dispersed and attenuated M-wave.

In real recordings, an additional noise term n(t) is generally considered, leading to the mor generic model

$$v(t) = K(t) * x(t) + n(t) \tag{3.3}$$

where *n(t)* represents measurement noise and minor deviations from the ideal assumptions.

This model forms the basis for the deconvolution process described in the following sections, where both the kernel and the delay distribution are estimated from experimental CMAP recordings.

3.1.1 Slow afterwave on CMAP

For the deconvolution method to work correctly, the kernel must reproduce the morphology of the compound muscle action potential (CMAP).
The CMAP shape is influenced by several physiological and technical factors, among which temperature and filter settings play a key role.
Cooling leads to prolonged depolarization and repolarization phases, due to slower Na^+/K^+ channel kinetics, resulting in increased latency, amplitude, area, and duration, together with a slower return to baseline. [13]

A crucial feature to include in the kernel is the slow afterwave (SAW) — a slow return to baseline following the main negative peak of the CMAP. Although it might appear as an artifact, the SAW

represents a physiological component that results from the slow repolarization phase of the intracellular action potential (IAP) [21].

The muscle fiber action potential can be divided into four stages: initiation, propagation, termination, and slow repolarization. The latter corresponds to a gradual negative afterpotential due to ionic processes in the T-tubular system. When multiple muscle fibers are activated simultaneously, the combined slow repolarization generates a low-frequency component that decays slowly toward baseline—precisely the SAW.

Improper filtering can distort the true CMAP waveform. The CMAP contains both low- and high-frequency components; thus, increasing the high-pass filter cut-off eliminates low-frequency content, attenuating the SAW and artificially shortening the waveform duration. For this reason, CMAPs are typically recorded with a bandwidth of 3 Hz–10 kHz, preserving the physiological low-frequency content necessary for accurate modelling [13].

The use of notch filters -50/60 Hz- during CMAP acquisition is generally not used, as they may introduce artifacts or attenuate adjacent frequency components, further altering waveform morphology.

Considering these aspects is essential when modelling the CMAP and its kernel, since the slow after wave is a physiological manifestation of slow membrane repolarization, not a recording artifact. Including it in the kernel ensures that the model correctly reproduces the true electrophysiological characteristics of muscle activation. In the implementation, the SAW is approximated as the product of an exponential decay and a sigmoid function, which together describe the attenuated repolarization tail following the main negative CMAP peak.

The exponential term is:

$$e(t) = A_1 e^{-A_2 t} \tag{3.4}$$

that models the temporal decay constant of the repolarization, while the sigmoid term

$$s(t) = \frac{1}{1 + e^{-a(t-c)}} \tag{3.5}$$

modulates the onset and smoothness of the transition back to the baseline.

Their product provides a representation of the slow after wave:

$$f_{\text{saw}}(t) = e(t) \cdot s(t) \tag{3.6}$$

as illustrated in the figure 3.1, where the interaction between exponential decay and sigmoid modulation can be clearly observed.

In the formula, A_1 defines the amplitude of the slow component, A_2 determines the decay rate-inversely related to the time constant of repolarization, while a and c control the slope and temporal

onset of the sigmoid. Together, these parameters allow flexible modelling of the low-frequency tail that characterizes the CMAP slow afterwave.

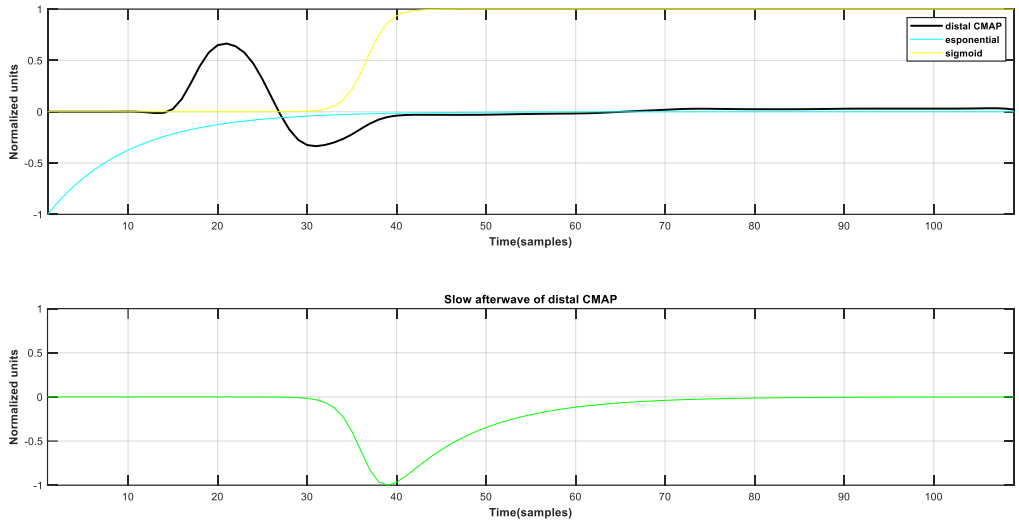

Figure 3.2 *Modelling of the slow after wave (SAW) as the product of an exponential decay and a sigmoid function. The exponential describes the repolarization time constant, while the sigmoid modulates the onset of the slow return to baseline.*

3.2 Basics of Deconvolution

Deconvolution is a mathematical technique used to separate overlapping signals into their original components. In the field of neurophysiology, this approach makes possible to interpret the recorded CMAP not as a single waveform, but as the sum of multiple delayed contributions from individual motor unit action potentials. By estimating the distribution of these conduction delays, deconvolution allows to distinguish true conduction block from the effects of temporal dispersion. In conventional nerve conduction studies, the presence of conduction block or temporal dispersion is usually inferred by comparing the amplitude or area of the CMAP recorded after distal and proximal stimulation. A substantial reduction in proximal amplitude compared to distal is interpreted as a conduction block, while more modest changes may reflect temporal dispersion. However, these parameters are strongly influenced by technical and physiological factors such as electrode placement, recording distance, temperature, and intrinsic variability of motor unit activation [4,11]. Even in normal subjects, a degree of amplitude loss or area reduction can occur with proximal stimulation, particularly in long nerves such as the tibial. This makes it difficult to distinguish physiological changes from pathological conduction block with certainty. Deconvolution techniques offer an advantage in this context. Instead of using amplitude or area ratios, it focuses on estimating the distribution of single-fiber conduction delays underlying the CMAP waveform. By separating the overlapping contributions of individual fibers, deconvolution allows a more accurate estimation of conduction delay and phase cancellation [19]. This makes it easier to tell the difference between an actual conduction block, where impulses cannot cross a nerve segment, and temporal dispersion, where the impulses are desynchronized. Thus, deconvolution reduces the confounding effects that limit traditional amplitude- and area-based

criteria and increases the sensitivity and specificity of conduction block detection. The relationship between the CMAP $v(t)$, the kernel $K(t)$, and the underlying delay distribution $x(t)$can be expressed as:

$$v(t) = \int_0^t K(t-\tau)\, x(\tau) d\tau$$

(3.7)

where $K(t)$ represents the stereotyped MUAP waveform, and $x(\tau)$ describes the distribution of conduction delays across activated motor fibers.

Solving equation 3.7 for x(t) given v(t) and K(t) constitutes an inverse problem. While computing the forward convolution (from x to y) is straightforward, the inverse operation is ill-posed: small perturbations in the recorded CMAP due to noise can lead to large, non-physiological oscillations in the estimated delay distribution. This instability necessitates the use of regularization techniques to obtain meaningful solutions. Direct minimisation of the mean-square error between the recorded and reconstructed CMAPs often leads to highly oscillatory and unstable estimates. In practical terms, this issue is addressed through Tikhonov regularisation, which introduces a residual norm to penalise unrealistic solutions. The regularised least-squares problem can include different penalty terms, such as:

$$\min_x \| Kx - v \|^2 + \alpha \| x \|^2$$

(3.9)

to suppress excessive amplitude oscillations, or

$$\min_x \| Kx - v \|^2 + \beta \| \nabla x \|^2$$

(3.10)

to smooth the estimated distribution by penalising rapid changes between adjacent samples. A combination of both terms (α + β) corresponds to a Tikhonov-type regularisation adapted for physiological data, balancing amplitude stabilisation with smoothness constraints and thus preventing the oscillations.

In practice, the convolution operation is discretised in matrix form, where the kernel *K* defines a Toeplitz convolution matrix and *x* represents the vector of delay amplitudes. The deconvolution problem is then expressed as a discrete linear inverse problem.

In matrix, the convolution can be expressed as:

$$\mathrm{v} = \mathrm{Kx}$$

(3.11)

where K is:

$$\mathrm{K} = \begin{bmatrix} k_1 & 0 & \cdots & 0 \\ k_2 & k_1 & \ddots & \vdots \\ \vdots & \ddots & \ddots & 0 \\ k_M & \cdots & k_2 & k_1 \end{bmatrix} \tag{3.12}$$

If the matrix K is square and well-conditioned, the inverse is possible; if itis rectangular or ill-conditioned, it cannot be inverted. For this reason, the deconvolution is performed by solving a regularised least-squares problem:

$$\hat{x} = arg \min_x \{||v(t) - K(t) * x(t)||^2 + \alpha||x(t)||^2\} \tag{3.13}$$

where the first term represents the residual norm, and the second term, the solution norm, penalises excessive amplitude oscillations. The Tikhonov regularisation problem can be expressed as:

$$\hat{x} = (K^T K + \alpha(I + F^T F))^{-1} K^T v \tag{3.14}$$

where F is the discrete first-derivative operator, used to penalise rapid variations between adjacent samples.
This formulation ensures that the estimated delay distribution is both smooth and numerically stable.

The deconvolution algorithm used in this work employs the Landweber iterative method to compute the regularised solution. While the Tikhonov formulation defines the objective function to be minimised, the Landweber algorithm provides an efficient iterative procedure to approach that solution through successive gradient-descent updates.

At each iteration k, the solution is updated according to the following formula:

$$x_{k+1} = x_k + \mu K^T (v - K x_k) \tag{3.15}$$

where μ is a relaxation parameter that controls the convergence speed.

The initial solution x_0 is obtained from the Tikhonov regularisation, and then iteratively refined through the Landweber algorithm in the direction of steepest descent of the error functional. The iterative update is followed by a projection step, which enforces the physiological constraints:

$$\begin{cases} v_{k+1} = x_k - \mu K^T (K x_k - v) \\ x_{k+1} = max(v_{k+1}, 0) \end{cases} \tag{3.16}$$

where the relaxation parameter μ is defined as:

$$\mu = \frac{0.9}{\lambda_{max}(K^T K)} \tag{3.17}$$

and chosen to ensure convergence in approximately ten iterations.

After each iteration, physiological constraints are applied: since conduction delays and motor-unit activations cannot be negative, a positivity constraint is enforced by setting negative values to zero. The support of *x(t)* is set in between a physiological range of conduction velocities (*CVmin–CVmax*), depending on the specific nerve under study.
In this way, the Landweber method acts as a constrained gradient-descent algorithm, refining the Tikhonov-regularised estimate while ensuring that the resulting delay distribution remains positive, and physiologically meaningful.

Having established the theoretical and numerical bases of deconvolution, as well as the regularisation and physiological constraints applied, the next section describes the procedure used to estimate the kernel function *K(t)* from experimental CMAP recordings and its application to the estimation of conduction block.

3.3 Kernel modelling

The kernel function K(t) defines the characteristic waveform of a motor unit action potential, and its accurate estimation is essential for reliable deconvolution.
In the implemented algorithm, the kernel is derived from the distal CMAP, recorded at the most distal stimulation site (typically at the wrist for upper limb nerves or at the ankle for lower limb nerves).
This choice is motivated by the fact that, distally, temporal dispersion is minimal, as conduction velocities have had less distance to diverge. Moreover, the distal response has a lower probability of conduction block and also exhibits a higher amplitude and signal-to-noise ratio (SNR) due to reduced phase cancellation and the proximity to the reference electrode.
This section explains how the kernel is modelled and optimized in the code, combining a Hermite polynomial representation with a physiologically inspired model of the slow afterwave (SAW).

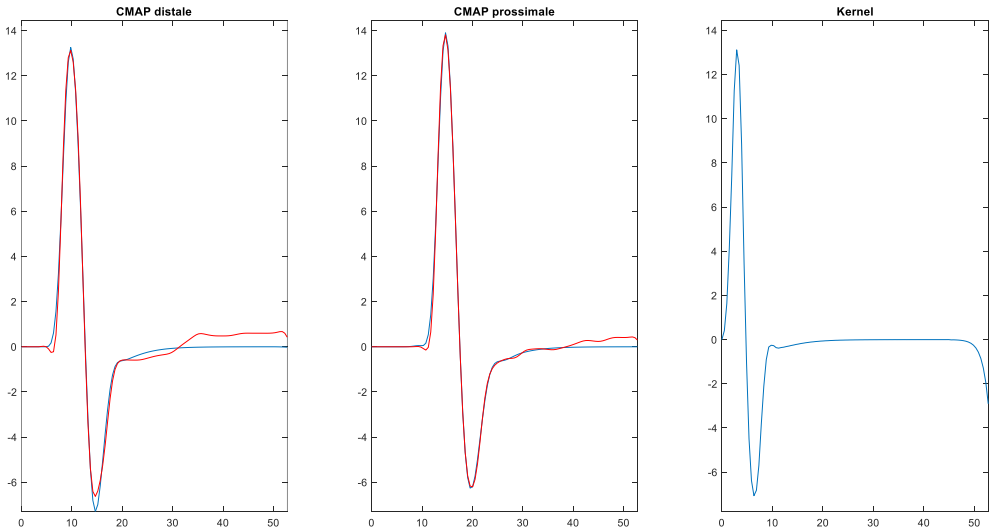

Figure 3.3 *Distal and proximal CMAPs together with the kernel used for deconvolution. The slow afterwave (SAW) appears as a slow return to baseline following the main negative peak and is included in the kernel model.*

The first step in kernel estimation consists in constructing an initial approximation of the MUAP waveform using a set of basis functions- in this case the Associate Hermite functions (AH). These functions form an orthogonal basis capable of capturing both the sharp and smooth transitions of action potentials, making them ideal for short, biphasic signals such as CMAPs.

The distal CMAP, $v_{\text{dist}}(t)$, is decomposed into a linear combination of N-Hermite functions, as shown in 3.18,

$$K(t) = \sum_{n=0}^{N} \beta_n \mu_{\lambda,n}(t) \tag{3.18}$$

where each basis function $\mu_{\lambda,n}(t)$is defined as:

$$\mu_{\lambda,n}(t) = \frac{1}{\sqrt{2^n!}} H_n\left(\frac{t}{\lambda}\right) \frac{1}{\pi^{1/4}\sqrt{\lambda}} e^{-\frac{t^2}{2\lambda^2}} \tag{3.19}$$

Here $H_n(t)$denotes the nth-order Hermite polynomial, recursively defined as:

$$H_0(t) = 1; H_1(t) = 2t; H_n(t) = 2tH_{n-1}(t) - 2(n-1)H_{n-2}(t) \tag{3.20}$$

The coefficients $\beta_n$control the relative contribution of each basis function, and λ is a scaling factor that adjusts the temporal width of the basis.

The number of Hermite functions N is selected to balance the computational accuracy and efficiency: in the practice, six to ten functions are sufficient to reproduce the main CMAP features. The Hermite-based model alone cannot reproduce the SAW. To model this physiological component, a slow term is added to the kernel, defined as the product of a decaying exponential and a sigmoid function, as said in section 3.1.1. The exponential term models the slow decay in time, while the sigmoid smooths the onset of the afterwave. The parameters of both functions are automatically tuned according to the morphology of the distal CMAP.
The resulting kernel thus combines a fast Hermite-based component (representing the main potential) and a slow exponential–sigmoid component (representing the SAW).

$$K_0(t) = K_{AH}(t) + f_{saw}(t)$$

(3.21)

Once the initial kernel is defined, an iterative optimization process is applied. At each iteration, the current kernel estimate is used to deconvolve both distal and proximal CMAPs. The reconstructed signals are compared to the experimental recordings, and the coefficients β_n are updated to minimize the mean squared error (MSE).

$$MSE[K] = ||v_{dist}(t) - K(t) * x_{dist}(t)||^2 + ||v_{prox}(t) - K(t) * x_{prox}(t)||^2$$

(3.22)

The kernel parameters are updated iteratively in the direction opposite to the gradient of the MSE:

$$p_{i+1} = p_i - \mu \frac{\nabla MSE}{|\nabla MSE|}$$

(3.23)

The optimization continues until the relative error E becomes smaller than 8% or the maximum number of iterations is reached. The error is defined as:

$$E = \frac{\sqrt{MSE[K]}}{\sqrt{||v_{dist}||^2 + ||v_{prox}||^2}}$$

(3.24)

After convergence, the optimized kernel provides a realistic and physiologically consistent representation of the MUAP waveform. From here the kernel is fixed and it is used to estimate the delay distribution.

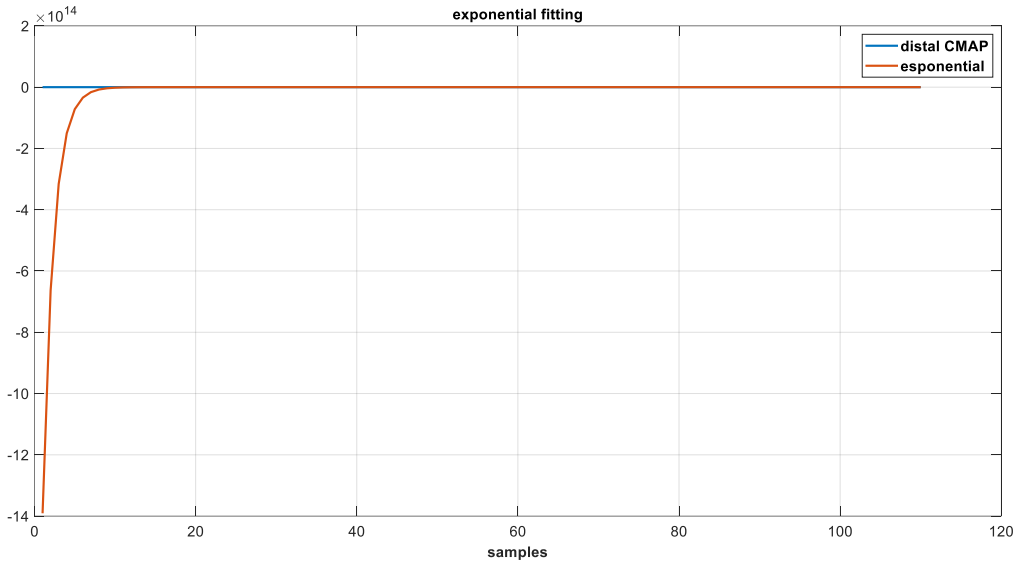

Figure 3.4 *Exponential fitting of the distal CMAP.*

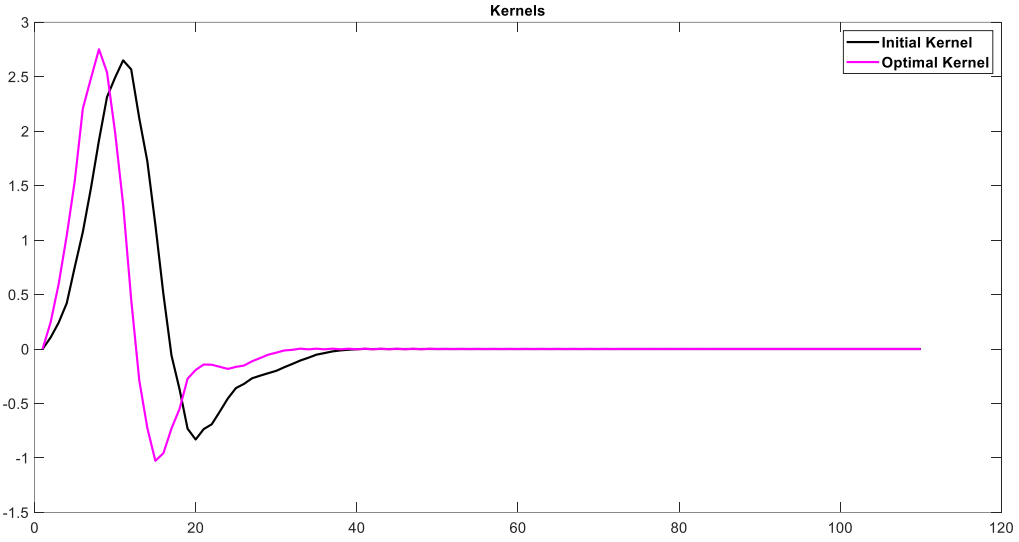

Figure 3.5 *Comparison between initial kernel (black) and optimal kernel (magenta).*

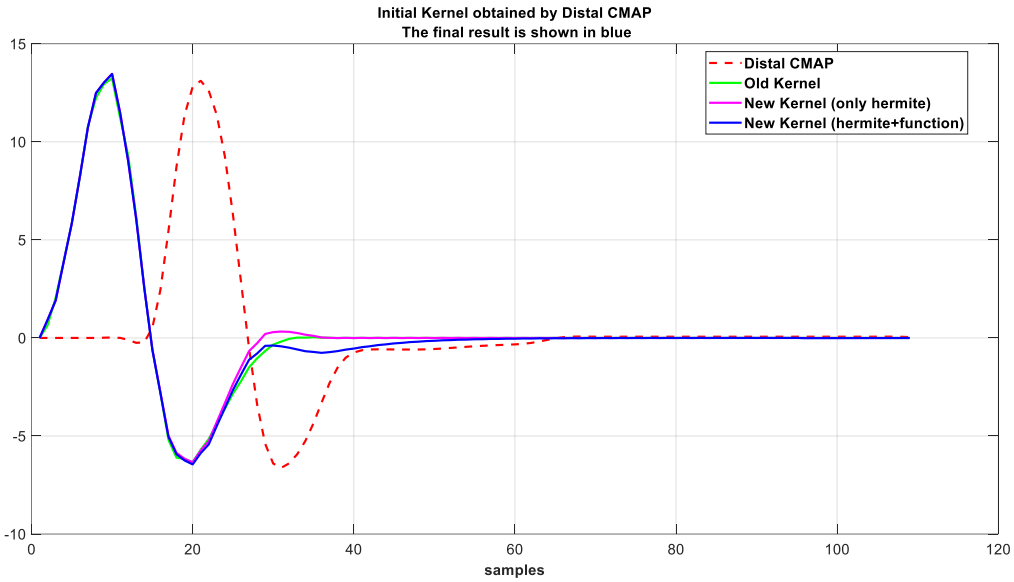

Figure 3.6 *Comparison between distal CMAP (red), old kernel (green), new kernel only with hermite (magenta) and new kernel with hermite+function (blue).*

The next section describes the implementation of this deconvolution process and the computation of the conduction block index.

3.4 Deconvolution algorithms: CB estimate from delay distributions

The presence of conduction block (CB) can be investigated by analyzing the distributions of delays of the motor unit action potentials (MUAPs) that contribute to compound muscle action potentials (CMAPs). Specifically, one can compare the delay distributions obtained from distal stimulation, x_{dist}, and proximal stimulation, x_{prox} . If conduction is intact, the two distributions should show comparable integrals, whereas the absence of some delayed responses in the proximal recording is indicative of a conduction block.

A mathematical formulation of this principle is expressed as:

$$CB = 1 - \frac{\int x_{prox}(t)dt}{\int x_{dist}(t)dt} \tag{3.25}$$

where the integrals of the delay distributions represent the total contribution of activated motor units at each stimulation site. The CB estimate is thus derived from the relative loss of MUAPs in the proximl distribution compared with the distal one.

Obtaining this estimate requires solving the convolution equation introduced in Section 3.1., i.e., reconstructing the delay distribution from the recorded CMAPs. Since this is an inverse problem, it is typically addressed through deconvolution techniques. In this context, the approach can be considered a form of "blind deconvolution," as both the kernel (representing the stereotyped MUAP shape) and the delay distribution must be estimated simultaneously.

Compared with conventional methods that depend only on amplitude or area ratios, the use of delay distributions provides a more robust assessment of CB. Traditional parameters are highly sensitive to temporal dispersion, which can mimic or obscure conduction block. By contrast, analyzing the delay distribution allows separation of phase cancellation effects from genuine loss of conduction, improving both sensitivity and specificity in CB detection.

Before performing the deconvolution and conduction block estimation, both distal and proximal CMAPs must be preprocessed to guarantee signal stability and make them directly comparable. A low-pass filter with a cutoff frequency of about 350 Hz removes high-frequency noise and slow baseline drifts. Because the onset and duration of CMAPs can differ slightly between stimulation sites, the signals are temporally aligned through cross-correlation to estimate and correct the relative delay between distal and proximal responses.

After filtering and alignment, both CMAPs are resampled to a common length and normalized in amplitude to ensure numerical stability during deconvolution. The processed signals are then used to estimate the kernel $K(t)$and the corresponding delay distributions $x_{dist}(t)$and $x_{prox}(t)$.

The following subsection provides an overview of the digitalisation process implemented at the beginning of the study to convert the acquired medical signals into a digital format suitable for further analysis.

3.5 Signals digitalisation procedure

The method was tested on experimental signals provided in the form of jpg images, extracted from the medical records of patients from various Italian hospitals and kindly made available by Dr. Cocito and Dr. Doneddu. The process followed to obtain these signals in digital format, necessary to test the proposed method, is described below.

Figure 3.7 shows a clinical image of a median nerve, in which two CMAPs are visible: the first, recorded at the wrist, represents the distal CMAP, while the second, recorded at the elbow, represents the proximal CMAP. Stimulation was performed using the electrode positioned on the APB (Abductor Pollicis Brevis) muscle as a reference. The image provides various useful pieces of information, including the number of time and amplitude divisions, as well as the corresponding values per division. Four reference points were identified: the first and fourth correspond to the

first and last markers, respectively, while the second and third identify the maximum peak of the positive phase and the minimum peak of the negative phase of the CMAP, respectively.

The image digitisation procedure was divided into several stages, integrated into a single operational flow. First, the image was rotated on the xy plane by estimating the angle formed by a line drawn between two points selected manually on the reference grid. Next, the isoelectric line was selected by identifying a point at the beginning of the CMAP useful for defining the baseline. Next, the vertical and temporal references were identified, which were necessary to determine the amplitude (in mV) and temporal duration of the CMAP, respectively. For both media, the user selected two corresponding points and entered the ms/Div and mV/Div values shown in the image to correctly calculate the temporal and amplitude scales of the signal.After this phase, the first and last markers were selected manually. The code was programmed to force all values prior to the first marker to zero in order to eliminate any artefacts or unwanted oscillations present before the onset of the CMAP. In a subsequent phase, an integrated MATLAB function was used to manually select the points on the trace; the pixel values thus obtained were then converted into voltage (mV) using the mV/Div scale shown in the image as a reference. The selected points were finally interpolated linearly with a sampling frequency of 2048 Hz, a value chosen to ensure a sufficiently smooth and accurate representation of the signal.

Figure 3.8 shows the manual interpolation of the selected points on a CMAP trace, while Figure 3.9 shows the digitised signal resulting from the process described.

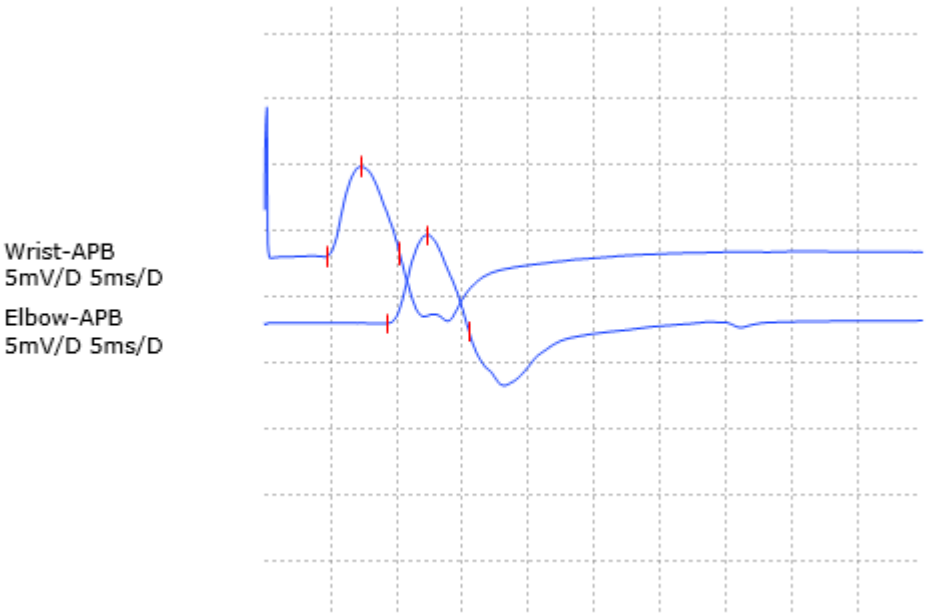

Figure 3.7 *Original trace from the medical records provided by neurologists.*

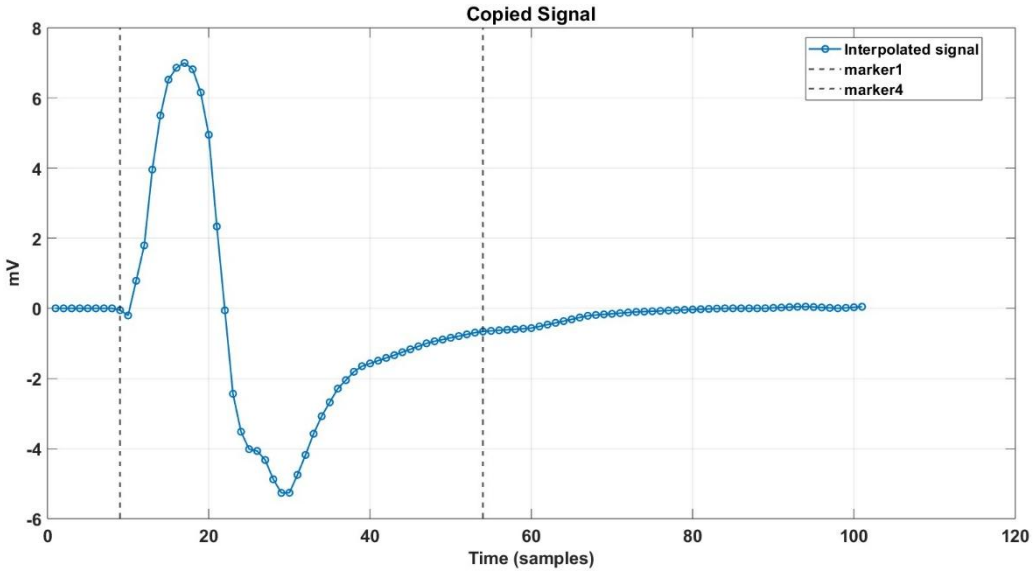

***Figure 3.8 Di**gitalised signal with the procedure described above.*

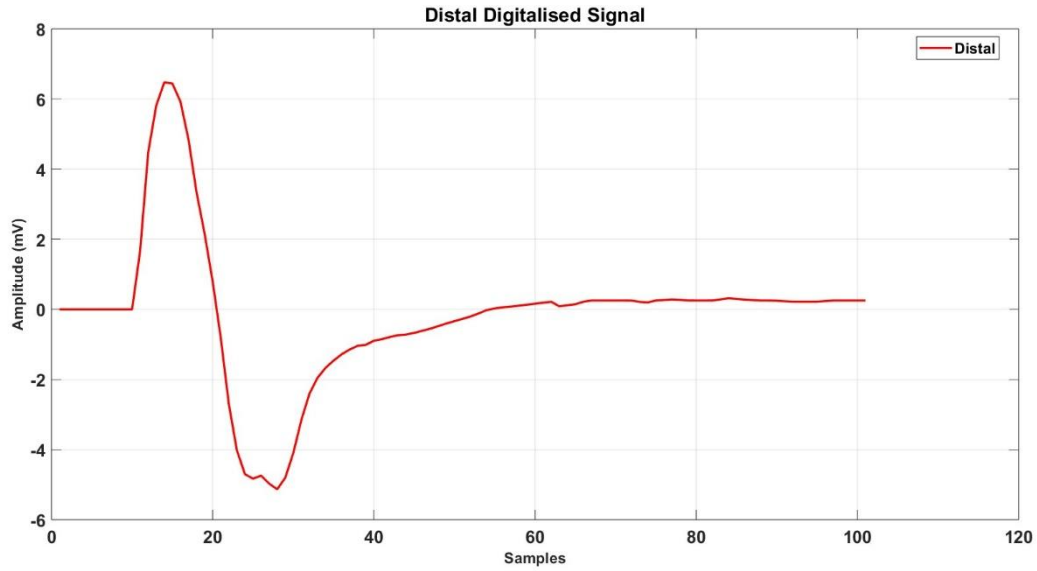

***Figure 3.9** Example of final digitalised signal.*

Chapter 4: Multicenter study-Methods and Results

This chapter show examples of CMAP recordings included and excluded in the analysis.

4.1 Healthy subject

In those figures we can see the tracings of healthy nerves.

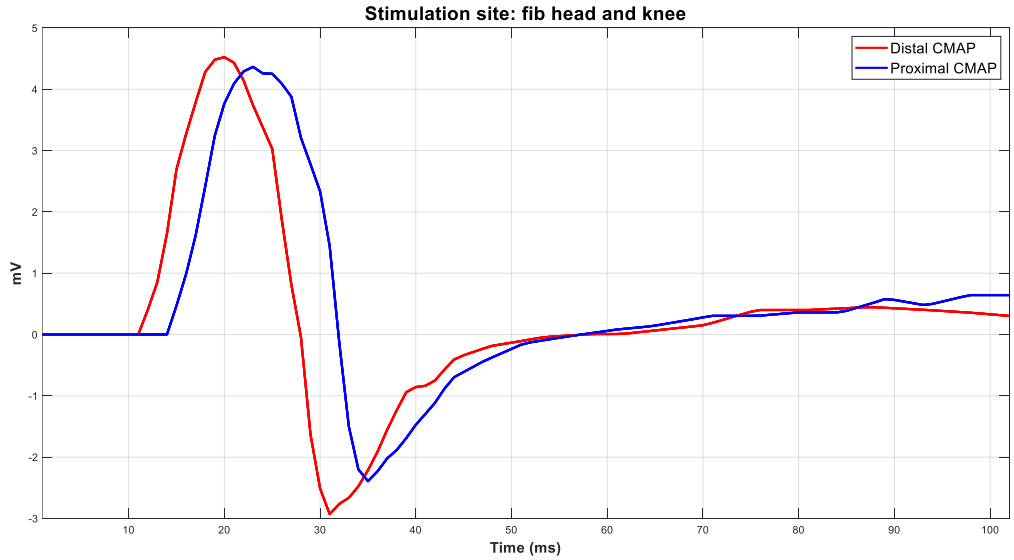

***Figure 4.1**: CMAP recorded by stimulating the peroneal nerve in the head of the fibula and the popliteal fossa. A distal distance of 100 mm and a proximal distance of 450 mm were set.*

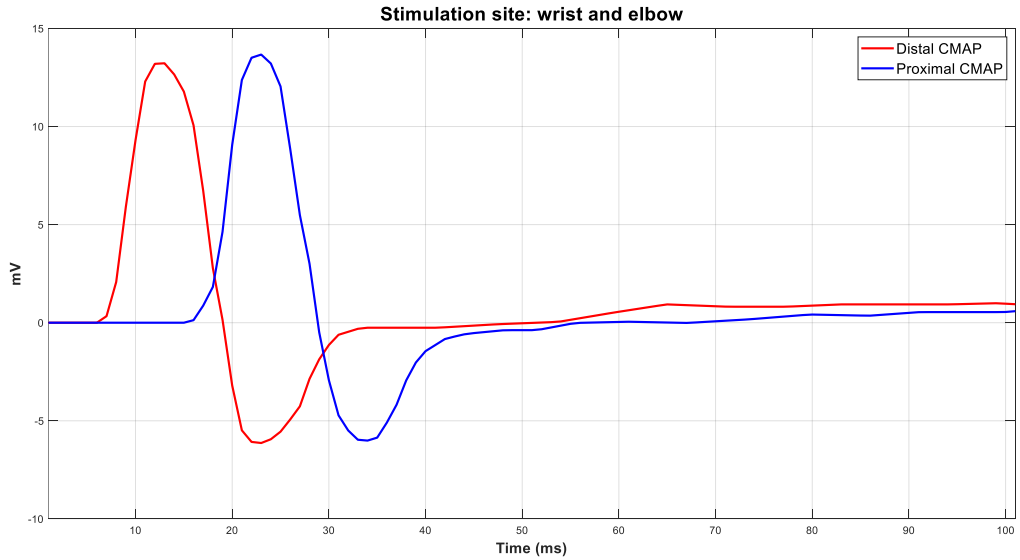

***Figure 4.2** CMAP recorded by stimulating the median nerve in wrist and elbow. A distal distance of 80 mm and a proximal distance of 250 mm were set.*

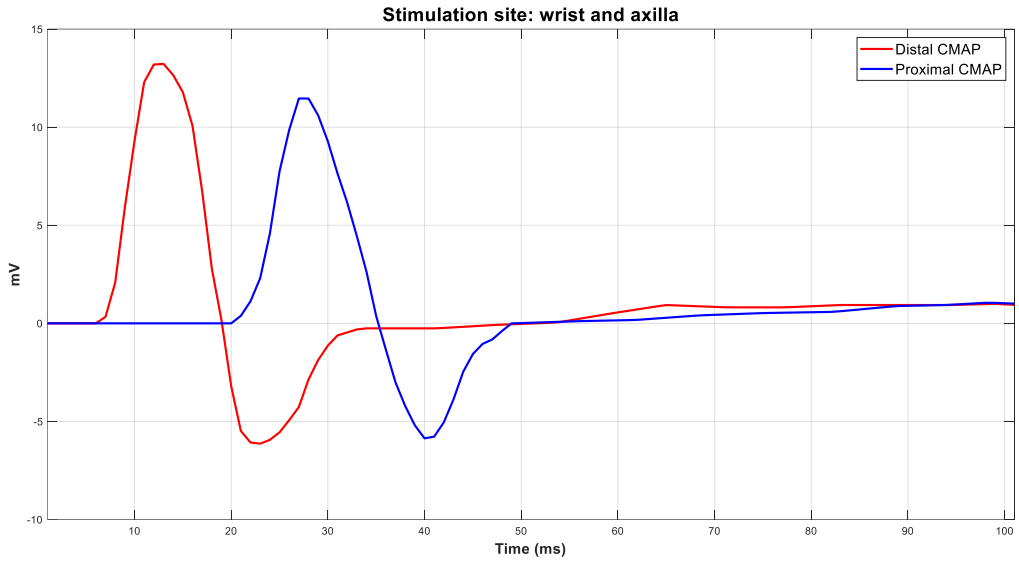

Figure 4.3 *CMAP recorded by stimulating the median nerve in wrist and axilla. A distal distance of 80 mm and a proximal distance of 330 mm were set.*

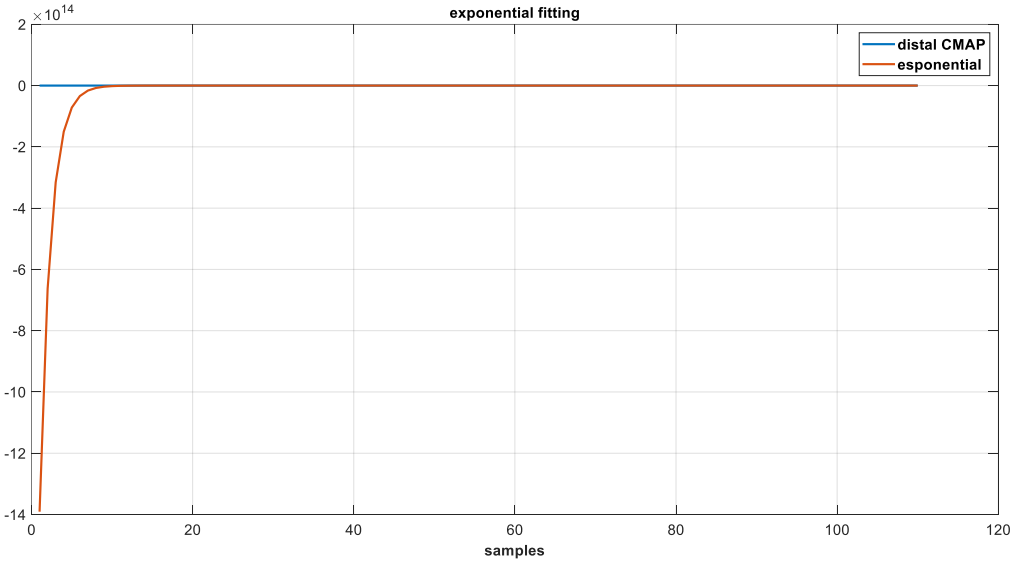

Figure 4.4 *The exponential fitting performed to model the return to baseline of the distal CMAP is shown.*

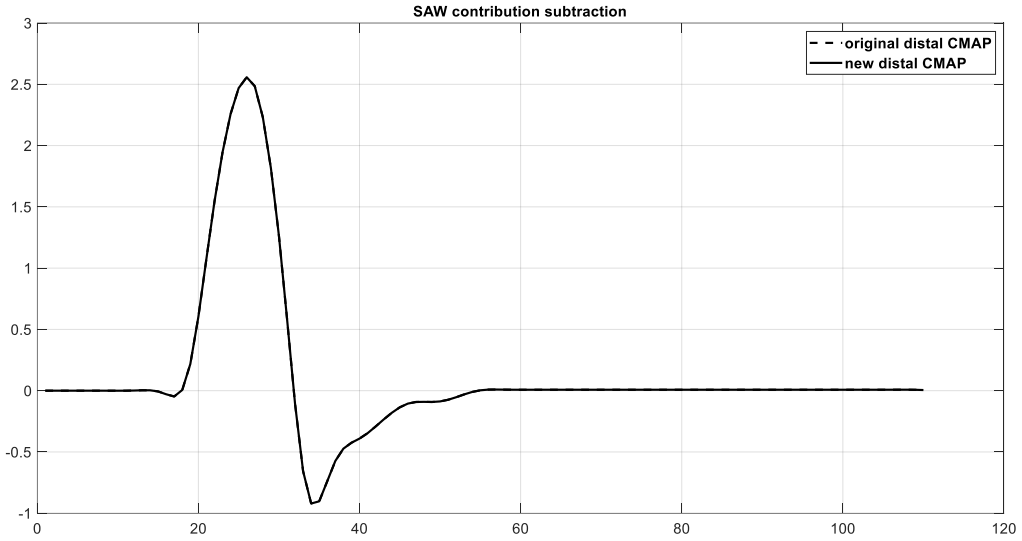

Figure 4.5 *The slow afterwave model appropriately reflects the negative phase and return to baseline of the distal CMAP.*

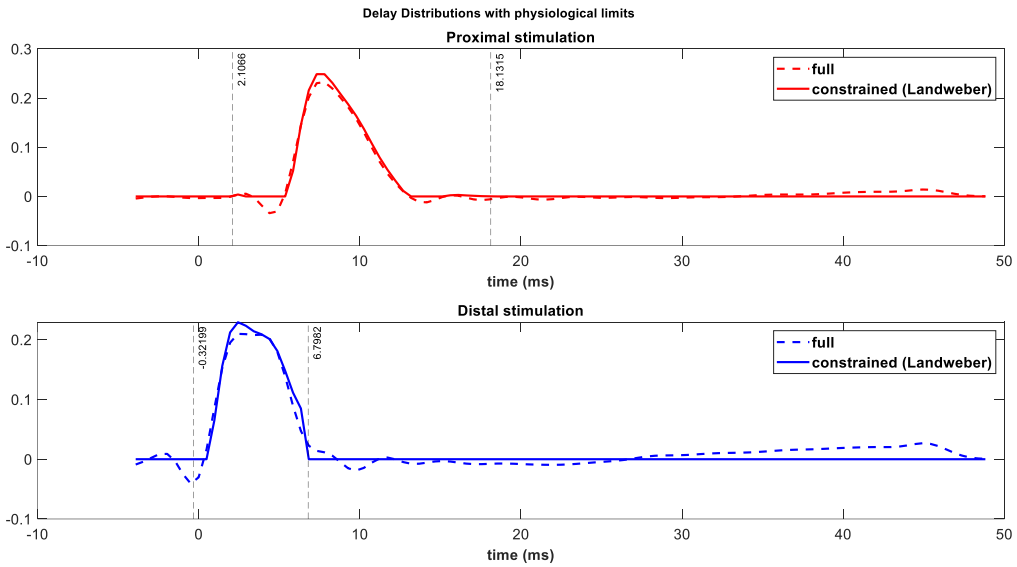

Figure 2.6 *This figure shows the Landweber reconstruction for both proximal and distal stimulation. It is possible to observe the high reconstruction accuracy, as the signal morphology is sufficiently well preserved.*

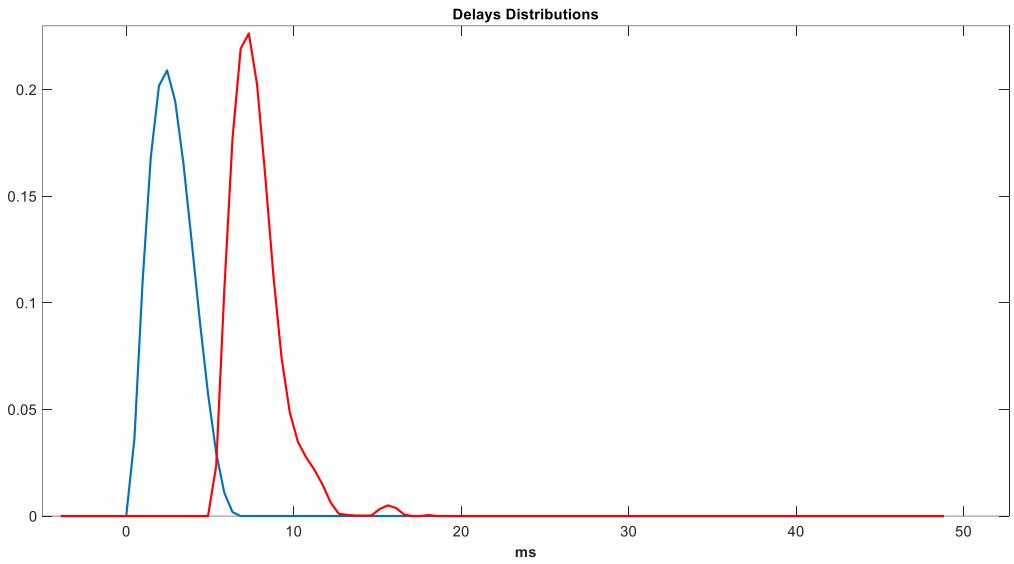

Figure 4.7 *The distribution of delays in the two CMAPs, distal (in blue) and proximal (in red), supports the theory of no conduction block. The proximal response partially intersects with the distal response, suggesting an almost immediate proximal response to the distal response.*

	Estimated Block
Deconvolution	-5.044 (Error reconstruction 9.7%)
Area	0.229
Amplitude	-5.296

Table 4.1 *Estimated values of CB for healthy subject*.

4.2: Pathological subjects

This section shows the results obtained on pathological subjects.

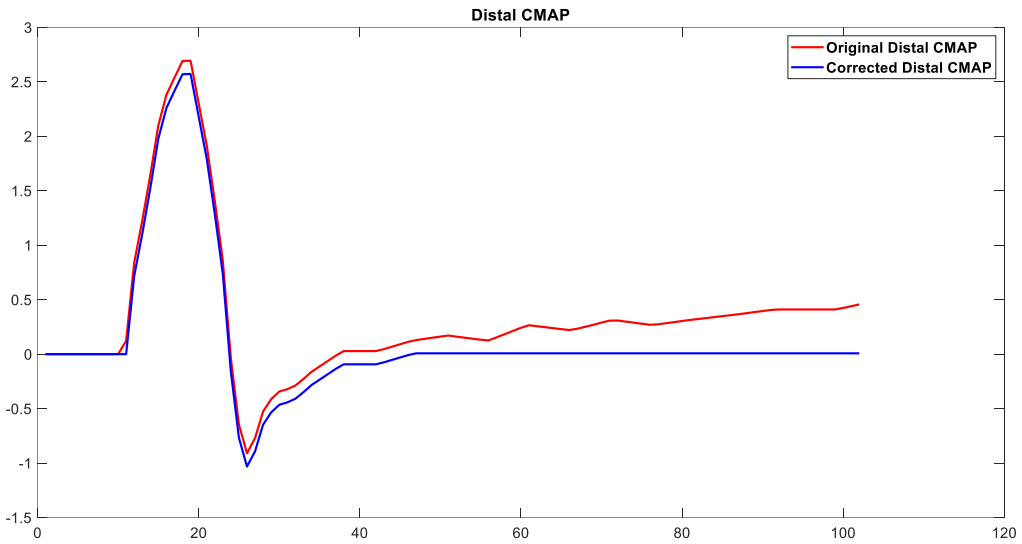

Figure 4.8 *In the figure above, both the baseline shift process and the removal of the final drift present in the original signal, which would have disrupted the proposed method, have been applied.*

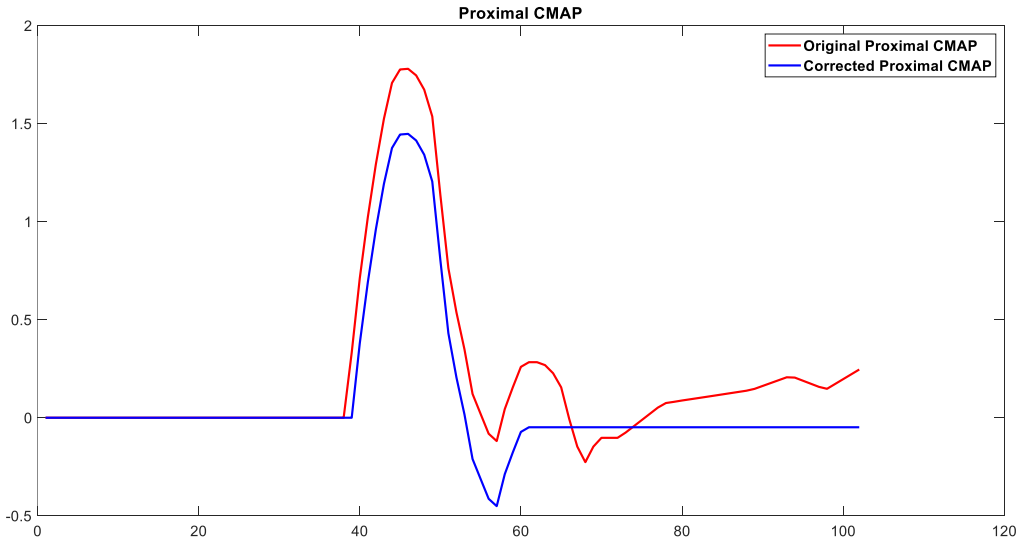

Figure 4.9 *The procedure described in Fig. 4.8 was also applied to the proximal CMAP.*

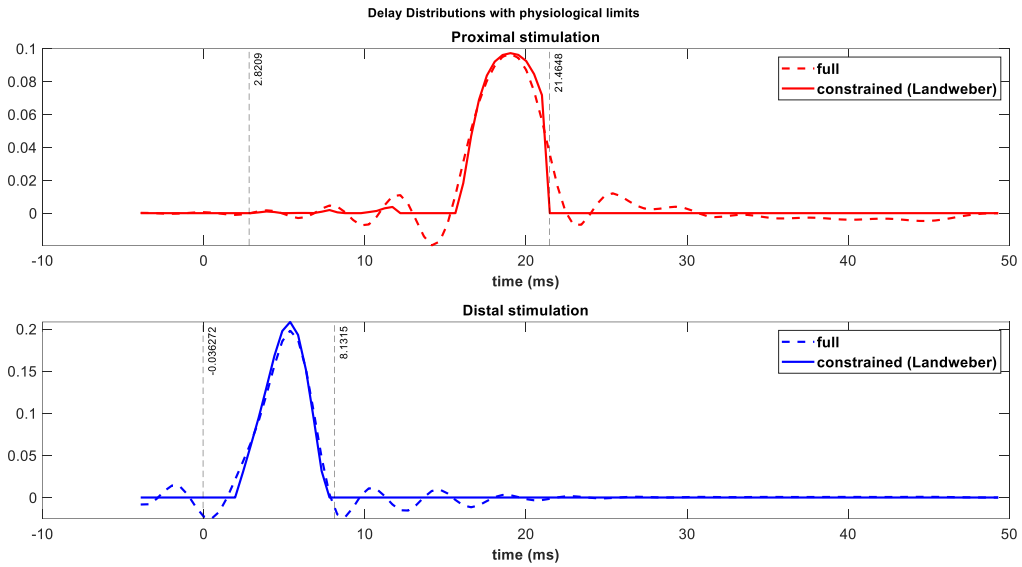

Figure 4.10 *This figure shows the Landweber reconstruction for both proximal and distal stimulation.*

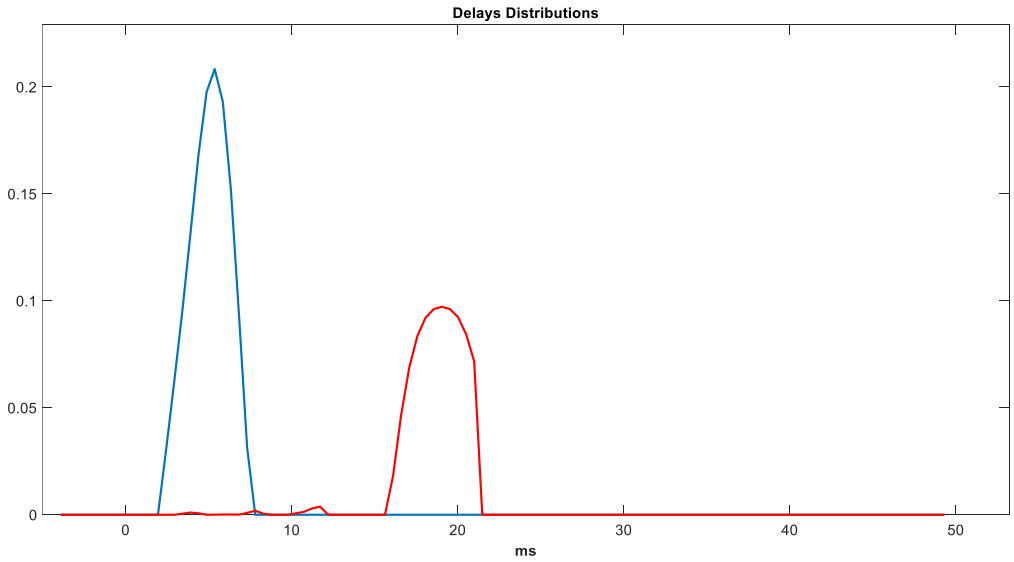

Figure 4.11 *The distal (blue) and proximal (red) delay distributions highlight the presence of conduction block, which, using the deconvolution method, can be seen in the delayed response of the proximal compared to the distal. With classical methods, a reduction in the area and amplitude of the proximal is noted, indicating the presence of CB. The best accuracy is obtained with the deconvolution method.*

	Estimated Block
Deconvolution	36.68 (Error reconstruction 9.5%)
Area	38.46
Amplitude	42.56

Table 4.2 *Estimated values of CB for pathological subject.*

4.3 Boxplot comparison

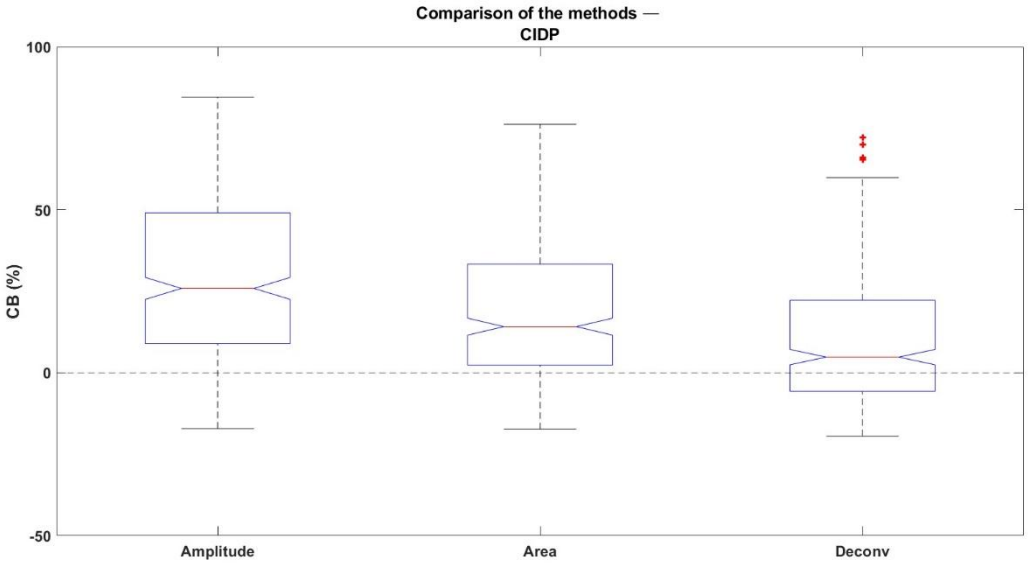

Figure 4.12 *Comparison of the estimated CB percentage using the amplitude, area, and deconvolution methods in CIDP patients. Each boxplot represents the distribution of CB values for each method.*

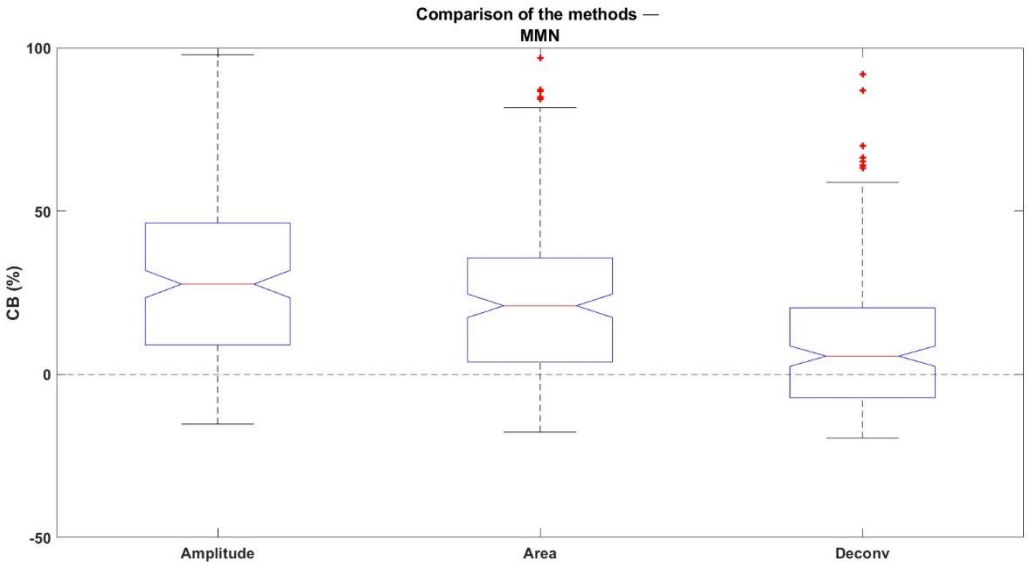

Figure 4.13 *Comparison of the estimated CB percentage using the amplitude, area, and deconvolution methods in MMN patients. Each boxplot represents the distribution of CB values for each method.*

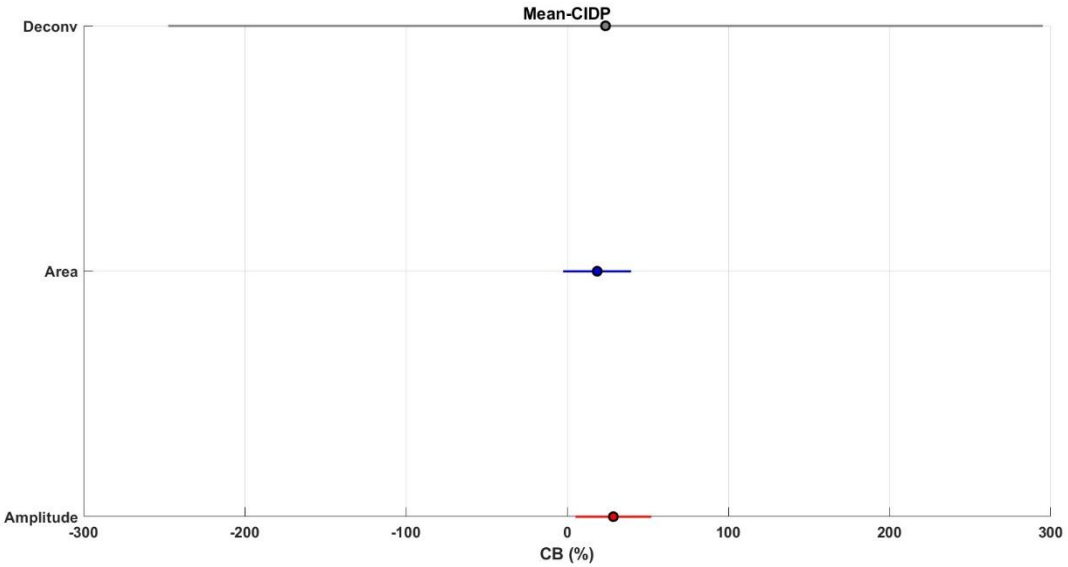

Figure 4.14 *Distribution of the estimated CB within the CIDP group across the three computational methods.*

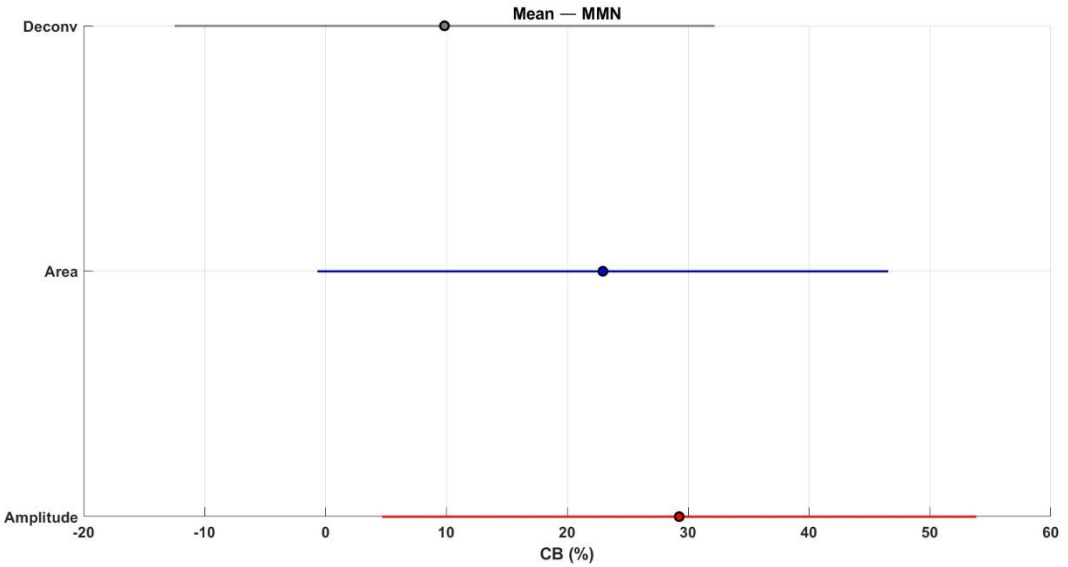

Figure 4.15 *Distribution of the estimated CB within the MMN group across the three computational methods.*

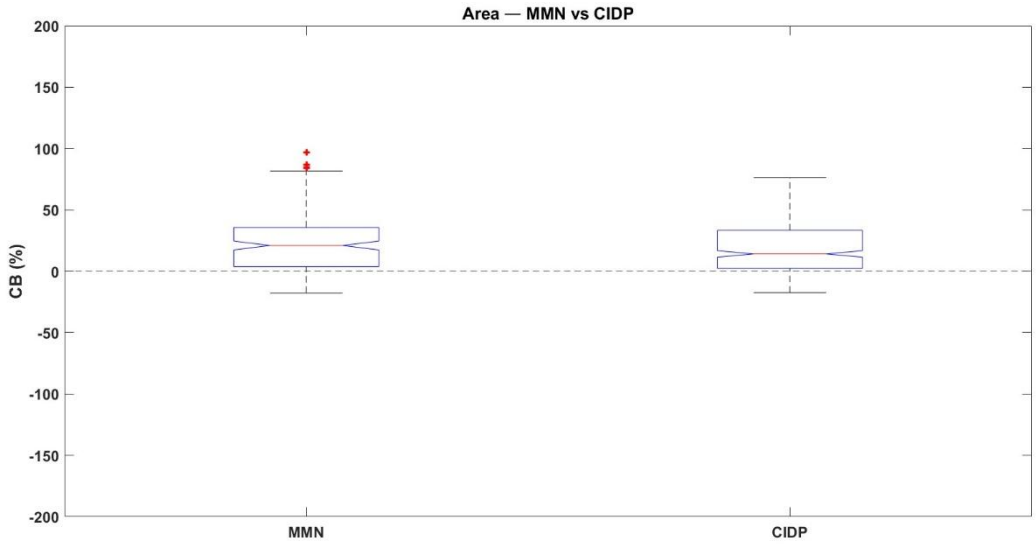

Figure 4.16 *Comparison of the CB for MMN and CIDP groups across area method.*

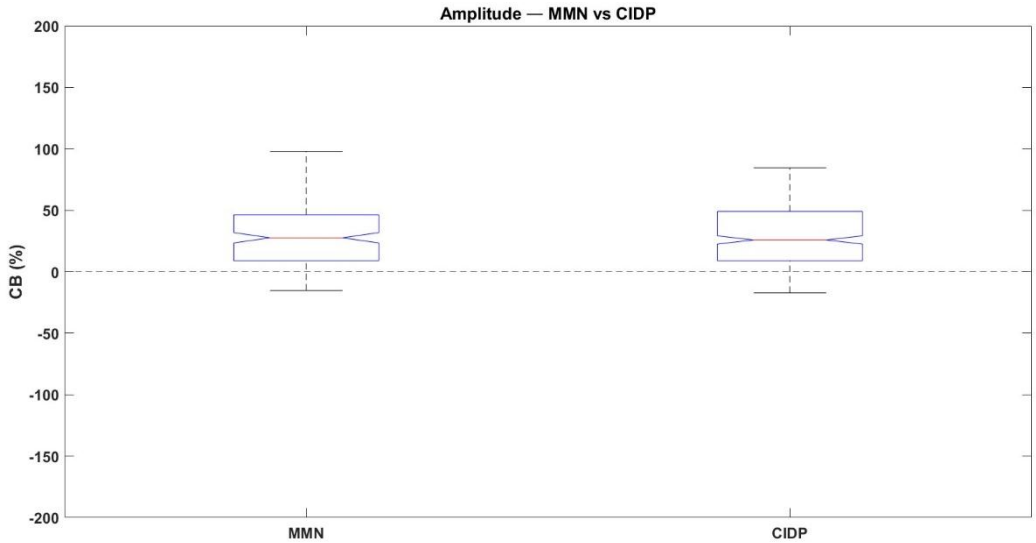

Figure 4.17 *Comparison of the CB for MMN and CIDP groups across amplitude method.*

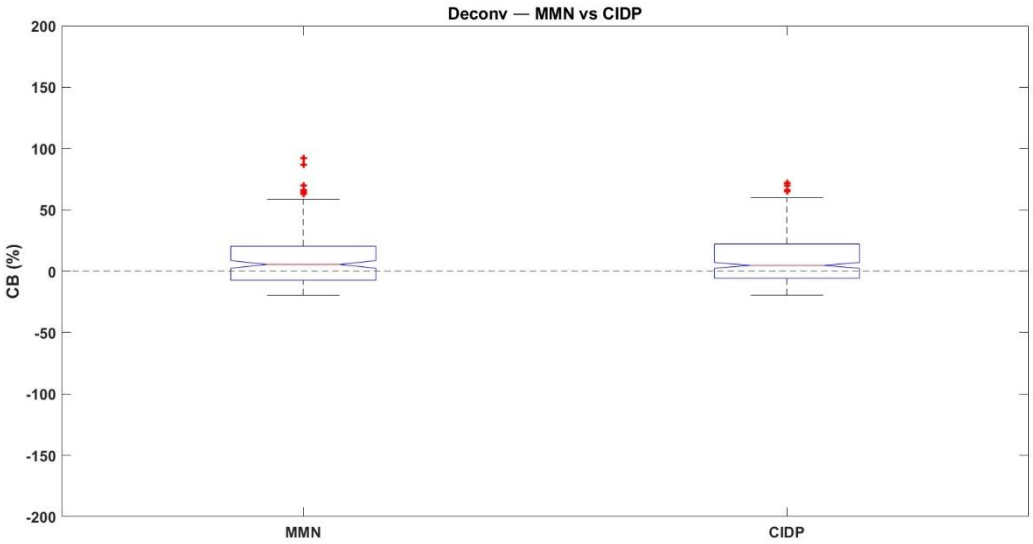

Figure 4.18 *Comparison of the CB for MMN and CIDP groups across deconvolution method.*

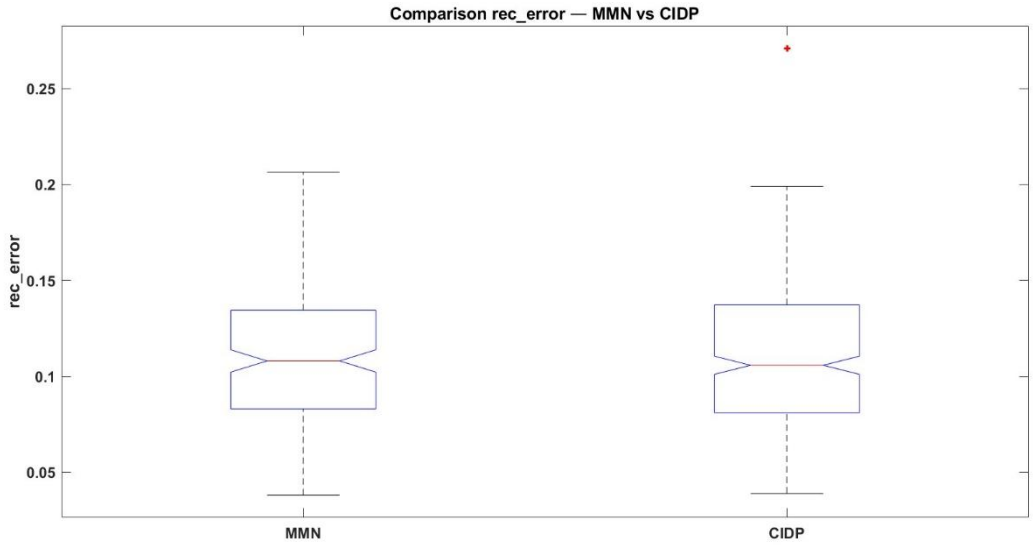

Figure 4.19 *Boxplot comparison of the reconstruction error between MMN and CIDP patients' groups.*

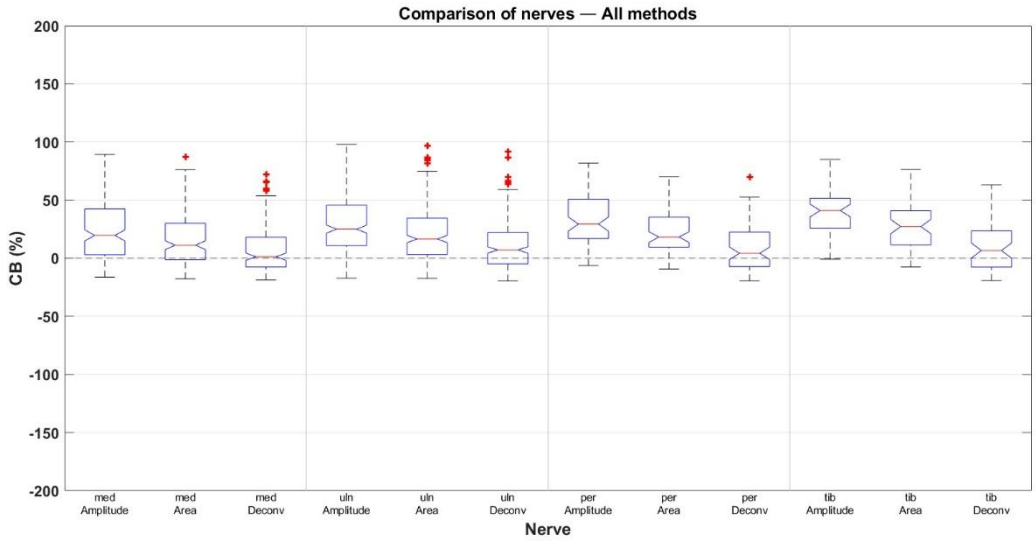

Figure 4.20 *Comparison of the CB across the different nerves – median, ulnar, peroneal, tibial- for the three computational methods*

Chapter 5: Discussion and conclusion

In this chapter the sensitivity of the proposed method to signal quality is discussed. Deconvolution represents an ill-posed inverse operation and is therefore extremely sensitive to acquisition conditions. Even minimal perturbations in the recorded trace, such as low-level noise or small artefacts, can lead to unstable delay distributions and non-physiological conduction estimates. This does not mean that there is a conceptual limitation of the method; rather, it highlights the need for highly standardized acquisition procedures to guarantee numerical stability and physiological plausibility.

5.1 Interpretation of the results

For each nerve, recordings were obtained at both distal and proximal stimulation points, considering additional anatomical reference sites when available (for example: wrist, below-elbow, and above-elbow for the ulnar nerve; wrist, elbow, axilla, and Erb's point for the median nerve; ankle and popliteal fossa for lower-limb nerves).

For each tracing three reduction indexes were computed (Landweber, area, and amplitude), together with the reconstruction error. Traces were included in the final analysis if they presented valid numerical values and coherent morphology across stimulati sites. Signals with undefined values or reconstruction error above the selected threshold were excluded.

The signals included in this multicenter dataset were derived from paper-based traces acquired in different hospitals with heterogeneous instrumentation and acquisition protocols. The dataset has been divided in two pathological classes:

- 116 patients with CIDP
- 42 patients with MMN

In addition, clinical documentation did not always explicitly specify the diagnostic status of each nerve within individual patients. In the absence of nerve-specific diagnostic information, it was assumed that traces exhibiting low or near-zero CB estimates corresponded to physiologically normal nerves. This assumption reflects the rationale that minimal or null reduction values are indicative of preserved motor fibre conduction and therefore suggest the absence of conduction block.

Then the digital reconstruction through point-by-point sampling introduces approximation in waveform morphology, particularly in low-amplitude components. As observed, this may reduce the stability of the algorithm under such conditions. For these reasons, direct digital acquisition would be preferable to obtain more reliable estimations, since paper traces introduce uncertainty. The absence of systematic digital archiving in clinical settings therefore represents a practical limitation for the implementation of the method

In some cases, essential acquisition parameters such as precise anatomical distances between stimulation points were missing, and standard distances were applied instead. Although this approach allows analysis to proceed, it may not be appropriate for all individuals, particularly those with significantly different limb lengths. In the first table below are reported the standard physiological distances between the stimulation sites used, where every value it is expressed in mm. In the second table below are reported the standard conduction velocity.

To estimate the CB, two CMAPs are required: a distal and a proximal response. In most of the available tracings, proximal stimulation was performed at multiple anatomical levels. For instance, in the median nerve of a given subject, distal stimulation may be applied at the wrist, while proximal stimulation may be applied at the elbow and also at the axilla. In such cases, the analysis for that nerve consists in evaluating both wrist-elbow and wrist-axilla CMAP pairs.

CB estimation with the proposed method requires specifying the anatomical distances between stimulation points as well as the minimum and maximum conduction velocities. In some recordings, these acquisition parameters were not available, therefore standard physiological values were used. Although this approach allows the analysis to proceed, it may not be appropriate for all individuals, particularly those with atypical limb lengths. The first table below reports the standard physiological distances between stimulation sites, expressed in millimetres, while the second table provides the corresponding reference conduction velocities.

Nerve	Distal	Proximal1	Proximal2	Proximal3
Median	80	250	330	400
Ulnar	80	260	370	470
Radial	80	310	400	-
Peroneal	110	420	550	650
Tibial	110	430	540	650
Femoral	250	500	650	-

Table 5.1 *Physiological distances between stimulation sites of every nerve analysed.*

Nerve	CV_{min}	CV_{max}
Median	15	70
Ulnar	15	70
Radial	10	70
Peroneal	10	70
Tibial	10	70
Femoral	10	70

Table 5.2 *Conduction velocity ranges for every nerve.*

The knowledge of these acquisition parameters has been essential during the deconvolution process. The minimum and maximum conduction velocities, as well as the distal and proximal distances, were initially set to standard physiological values. However, in the presence of pathological conditions, these ranges were deliberately widened or narrowed to allow the algorithm to converge and reconstruct an interpretable delay distribution. This adjustment became necessary because many patients exhibited markedly reduced conduction velocities, consistent with demyelinating neuropathies. Without extending the admissible velocity range, the inversion algorithm would have produced unstable results or failed to converge, since the predefined physiological constraints would have excluded the pathological conduction spectrum.

In most of the data available to us, the positive phase of the CMAP was not preceded by exactly zero values, but by values that generated slight negative or positive peaks associated with artefacts. This resulted in Landweber estimates that were not entirely accurate, as these artefacts interfere with the algorithm itself. Consequently, it was decided to apply a signal shift so that the first sample identifying the positive phase of the CMAP was preceded by zero values, thus creating a near-perfect trace.

In several signals obtained from paper tracings, a slow baseline drift was observed, as can be seen in Fig.4.8 Since the current implementation does not automatically compensate for baseline deviations, this phenomenon can affect the stability of the reconstruction. For this reason, a code was implemented to eliminate this slow drift, which in some cases produced NaN values due to the impossibility of performing exponential fitting and in others gave consistent Landweber estimates but with high reconstruction error. To remove the drift present in the late phase of the signal, a post-event saturation procedure was adopted. In particular, for each trace, the first sample intersecting the baseline after the negative peak of the CMAP was identified. This sample represents the point at which the physiological response ends and the signal, under ideal conditions, should return to the baseline. Starting from this point, all subsequent samples were forced to the value of the intersection sample, thus producing a constant final section, as can be seen in Fig.4.9. This operation allows the elimination of residual non-physiological drift. In some subjects, the slow drift of the baseline included oscillations Fig.4.9 which were removed along with it. In these cases, the morphology of the initial signal was not preserved, but Landweber's estimation of the CB was improved.

In Fig.4.12 and Fig.4.13 are represented boxplots of the CB distribution corresponding respectively to CIDP and MMN, and as it can be seen in the images the deconvolution method estimates better since it is less sensible to phase cancellation, effect that is even more pronounced in pathological nerves due to temporal dispersion. In contrast, the amplitude and area methods tend to overestimate the conduction block compared with deconvolution.

Furthermore, Figures 4.14 and 4.15 show that, for both CIDP patients and those diagnosed with MMN, the estimated mean CB value is systematically lower when calculated using the deconvolution method than when calculated using standard clinical methods. For CIDP patients, the mean CB is very close to that estimated using the area. This is due to the variety of data and the exclusion of CB values estimated above -30 using the proposed method. This result provides further confirmation of the effectiveness of the proposed method in more accurately compensating

for the effects of phase cancellations, which are often responsible for underestimating signal components.

Another interesting element, highlighted by the figures themselves, concerns the difference between the two groups of patients: the average estimated CB for subjects with CIDP is higher overall than that obtained for MMN patients, regardless of the estimation method used. This evidence could represent a potential key to differentiating between the two diseases, suggesting that quantitative analysis of CB alone could help support differential diagnosis in clinical settings.

The differences between CIDP and MMN can be better visualised in Fig. 4.16–4.18 where is represented their direct comparison for the three methods. CIDP patients present a wider spread of values and a higher variability, that is consistent with the fact that the demyelination in this disease is symmetric for the nerves, causing a greater temporal dispersion and partial conduction blocks. On the other side, MMN patients show a more concentrated and asymmetric distribution of CB values, which is in line with the multifocal nature of the disease described in 2.1.

Comparing the reconstruction error of the method between patients with CIDP and MMN, the boxplots in Figure 4.19 show that the error remains low overall, with values below 25%. Furthermore, the boxplots show that, in pathological cases of MMN, the reconstruction error is on average lower than that of patients with CIDP. This result is particularly interesting, as a lower reconstruction error implies signals with better morphology, which is totally in line with the previously discussed physiological differences between the two neuropathies. In CIDP, CMAPs tend to appear wider and more distorted due to the higher temporal dispersion, whereas in MMN, the signals are generally more compact and regular. Consequently, this could suggest that subjects with MMN have overall better CMAPs from a morphological point of view than those recorded in patients with CIDP.

Figure 4.20 shows a comparison between the different nerves analysed and the estimates obtained using the three methods considered. Here too, the deconvolution method shows overall greater accuracy than the area- and amplitude-based methods, which tend to underestimate CB values. Furthermore, the boxplots show that, for the peroneal and tibial nerves, the CB estimates obtained with the proposed method are lower than those for the ulnar and median nerves. This difference could be attributed to the lower availability of CMAPs recorded on the peroneal and tibial nerves, which may affect the quality of the estimate and the stability of the reconstruction process.

5.2 Strengths and limitations of the proposed method

The algorithm demonstrated excellent behaviour on synthetic signals and clean clinical recordings, confirming the theoretical validity of the approach. These results confirm the theoretical validity of the approach and its ability to reconstruct the physiological properties of the muscle response. In particular, the analysis of the presented boxplots shows that the method yields lower CB estimates compared to conventional clinical techniques, suggesting a greater capability to compensate for the effects of phase cancellation

Although the method proves generally effective, certain limitations emerge when dealing with realistic and complex signals. These limitations are not attributable to the theoretical formulation of the model, but rather to the quality and morphology of the input CMAP. The reconstruction

produced by the method is indeed sensitive to waveform morphology. When the CMAP deviates substantially from the expected biphasic shape, for example due to multiple late positive peaks or non-physiological post-peak oscillations, the fitting procedure may yield suboptimal reconstructions, resulting in distorted CB estimates.

Another critical factor is the presence of a marked positive drift at the end of the signal, a phenomenon likely caused by electrode–skin instability, impedance fluctuations, or movement artefacts. This drift is not representative of the physiological return to baseline of the CMAP, and consequently, the reconstruction error tends to increase significantly. To address this issue, the procedure described in the previous paragraph was implemented, enabling attenuation of the drift effect and improving both the CB estimate and the reconstruction error returned by the method.

Movement and stimulation artefacts represent an additional limitation of the method. Signals affected by such artefacts tend to be interpreted by the algorithm as physiologically meaningful components and are therefore incorporated into the reconstruction. This leads to unreliable CB estimation. For this reason, a baseline-shifting procedure was applied, as previously discussed.

Supramaximal stimulation is essential to guarantee complete motor unit recruitment and to avoid artefactual reduction in CMAP amplitude. When stimulation remains submaximal, which may occur for patient-tolerance reasons, only a fraction of motor fibres is activated, and the resulting waveform may falsely mimic conduction block or exaggerated temporal dispersion. A similar problem arises in the presence of mechanical disturbances during acquisition. Even minimal limb movements modify the electrode–tissue interface and alter CMAP morphology, introducing fluctuations in amplitude and baseline that propagate into the deconvolution process and ultimately bias delay-distribution estimation. For this reason, strict mechanical stabilization of the limb during stimulation is required to preserve the integrity of the recorded waveform.

Thus, the method is reliable and stable when applied to signals whose morphology is similar to a physiological biphasic CMAP, recorded under controlled conditions with minimization of movement artefacts (therefore suggesting limb immobilization), adequate electrode stabilization, and correct adjustment of stimulation intensity.
Under these conditions, the proposed method yields an accurate estimation of CB and shows reduced susceptibility caused by phase cancellation or systematic artefacts.

5.3 Conclusions

In this work, the innovative method for CB estimation introduced in [19] was further developed and applied to experimental signals. The dataset was divided into CIDP and MMN, corresponding to the pathologies diagnosed in the patients from whom the recordings were obtained.

The deconvolution method presented can only be applied to CMAPs with a biphasic morphology, which is why CMAPs composed of polyphasic MUAPs were excluded.

Considering the results previously discussed, the method has proven to be more diagnostically accurate in the estimation of CB. Furthermore, it has been shown that some limitations of traditional clinical methods, which rely exclusively on comparing area and amplitude between distal and proximal stimulation, have been overcome. Among these, a key limitation was the inability to compensate for phase-cancellation effects. The proposed method demonstrated robustness in compensating for these effects, indicating increased sensitivity in detecting the presence of CB.

Application of the method to a large multicentre dataset enabled testing under realistic conditions. The results highlighted that signal quality is critical for reliable reconstruction. Specifically, movement artefacts, electrode-skin instability, baseline drift, and the presence of non-physiological late components all influenced inversion convergence and estimation accuracy. These factors required the implementation of dedicated pre-processing procedures, such as signal shifting and post-event saturation, which significantly improved numerical stability and reconstruction error.

Despite challenges associated with signal quality, the method demonstrated promising clinical potential, offering strong performance when appropriate acquisition conditions, supramaximal stimulation, and artefact minimization are ensured. This suggests that systematic digital archiving of electrophysiological data is a necessary requirement to guarantee robust performance of the method.

In conclusion, the proposed method represents a significant contribution to qualitative nerve conduction analysis, providing an advanced strategy for CB estimation.

Bibliography

[1] Peter J. Bazira, An overview of the nervous system, Surgery (Oxford), Volume 39, Issue 8, 2021, Pages 451-462, ISSN 0263-9319, https://doi.org/10.1016/j.mpsur.2021.06.012. (https://www.sciencedirect.com/science/article/pii/S0263931921001411)

[2] Purves D, Augustine GJ, Fitzpatrick D, et al., editors. Neuroscience. 2nd edition. Sunderland (MA): Sinauer Associates; 2001. Increased Conduction Velocity as a Result of Myelination. Available from: https://www.ncbi.nlm.nih.gov/books/NBK10921/

[3] Olmo MD, Domingo R. EMG Characterization and Processing in Production Engineering. Materials (Basel). 2020 Dec 20;13(24):5815. doi: 10.3390/ma13245815. PMID: 33419283; PMCID: PMC7766856.

[4] Mallik A, Weir AI. Nerve conduction studies: essentials and pitfalls in practice. J Neurol Neurosurg Psychiatry. 2005 Jun;76 Suppl 2(Suppl 2): ii23-31. doi: 10.1136/jnnp.2005.069138. PMID: 15961865; PMCID: PMC1765692.

[5] Kane NM, Oware A. Nerve conduction and electromyography studies. J Neurol. 2012 Jul;259(7):1502-8. doi: 10.1007/s00415-012-6497-3. Epub 2012 May 22. PMID: 22614870.

[6] Shy ME, Jáni A, Krajewski K, Grandis M, Lewis RA, Li J, Shy RR, Balsamo J, Lilien J, Garbern JY, Kamholz J. Phenotypic clustering in MPZ mutations. Brain. 2004 Feb;127(Pt 2):371-84. doi: 10.1093/brain/awh048. Epub 2004 Jan 7. PMID: 14711881.

[7] Preston DC, Shapiro BE. Electromyography and Neuromuscular Disorders: Clinical-Electrophysiologic Correlations. 4th ed. Philadelphia: Elsevier; 2020. p. 33-41.

[8] Kimura J. Electrodiagnosis in Diseases of Nerve and Muscle: Principles and Practice. 4th ed. New York: Oxford University Press; 2013. p. 95-112.

[9] Abdalbary SA, Abdel-Wahed M, Amr S, Mahmoud M, El-Shaarawy EAA, Salaheldin S, Fares A. The Myth of Median Nerve in Forearm and Its Role in Double Crush Syndrome: A Cadaveric Study. Front Surg. 2021 Sep 21; 8:648779. doi: 10.3389/fsurg.2021.648779. PMID: 34621777; PMCID: PMC8490666.

[10] John C Kincaid. «The compound muscle action potential and its shape». In: Muscle and Nerve 22.1 (1999), pp. 4–5 (cit. on p. 7).

[11] Adrichem ME, Eftimov F, van Schaik IN. Intravenous immunoglobulin treatment in chronic inflammatory demyelinating polyradiculoneuropathy, a time to start and a time to stop. J Peripher Nerv Syst. 2016 Sep;21(3):121-7. doi: 10.1111/jns.12176. PMID: 27241239.

[12] Stålberg E, Karlsson L. The motor nerve simulator. Clin Neurophysiol. 2001 Nov;112(11):2118-32. doi: 10.1016/s1388-2457(01)00672-1. PMID: 11682351.

[13] Barkhaus PE, Nandedkar SD, de Carvalho M, Swash M, Stålberg EV. Revisiting the compound muscle action potential (CMAP). Clin Neurophysiol Pract. 2024 May 8; 9:176-200. doi: 10.1016/j.cnp.2024.04.002. PMID: 38807704; PMCID: PMC11131082.

[14] https://www.humanitas.it/news/neuropatia-periferica-quali-sono-i-sintomi/

[15] https://continentalhospitals.com/it/diseases/demyelinating-neuropathy/

[16] https://www.sciencedirect.com/science/article/abs/pii/S1388245720304296

[17] Feasby TE, Brown WF, Gilbert JJ, Hahn AF. The pathological basis of conduction block in human neuropathies. J Neurol Neurosurg Psychiatry. 1985 Mar;48(3):239-44. doi: 10.1136/jnnp.48.3.239. PMID: 3981192; PMCID: PMC1028257

[18] Kimura J. Facts, fallacies, and fancies of nerve conduction studies: twenty-first annual Edward H. Lambert Lecture. Muscle Nerve. 1997 Jul;20(7):777-87. doi: 10.1002/(sici)1097-4598(199707)20:7<777: aid-mus1>3.0.co;2-4. PMID: 9179149.

[19] Mesin L, Cocito D. A new method for the estimation of motor nerve conduction block. Clin Neurophysiol. 2007 Apr;118(4):730-40. doi: 10.1016/j.clinph.2006.11.015. Epub 2007 Feb 21. PMID: 17317295.

[20] Schulte-Mattler WJ, Müller T, Georgiadis D, Kornhuber ME, Zierz S. Length dependence of variables associated with temporal dispersion in human motor nerves. Muscle Nerve. 2001 Apr;24(4):527-33. doi: 10.1002/mus.1036. PMID: 11268025.

[21] Lateva ZC, McGill KC. The physiological origin of the slow afterwave in muscle action potentials. Electroencephalogr Clin Neurophysiol. 1998 Oct;109(5):462-9. doi: 10.1016/s0924-980x(98)00048-4. PMID: 9851304.